Joint Device Pairing, Reflection Coefficients, and Power Control for NOMA Backscatter Systems

Farhad Dashti Ardakani, Rui Huang, *Student Member, IEEE*, and Vincent W.S. Wong, *Fellow, IEEE*

***Abstract*—Non-orthogonal multiple access (NOMA) and backscatter communication are two emerging technologies for low-power communication. In this paper, we consider a NOMA backscatter system, where signals from two backscatter devices are multiplexed on a frequency resource block using NOMA in each time slot. Our objective is to maximize the average energy efficiency by optimizing backscatter device pairing, reflection coefficients of backscatter devices, and the transmit power of the reader. We formulate the average energy efficiency maximization problem subject to the minimum circuit power and the minimum data rate requirements of the backscatter devices, and the transmit power constraint of the reader. The formulated problem is nonconvex. To obtain a suboptimal solution for this problem, we use alternating optimization technique and decompose the problem into two subproblems. The subproblems are solved by using fractional programming, Dinkelbach's algorithm, and successive convex approximation method. Simulation results show that our proposed algorithm converges quickly to a suboptimal solution. Our proposed algorithm outperforms several baseline algorithms, including the genetic algorithm, fixed device pairing scheme, conventional device pairing scheme, maximum transmit power allocation scheme, and random reflection coefficient selection scheme, in terms of the average energy efficiency. The optimality gap of our proposed algorithm is investigated by comparing with the optimal scheme, in which the optimal device pairing is obtained based on exhaustive search.**

***Index Terms*—Energy efficiency, non-orthogonal multiple access, backscatter communication, alternating optimization, fractional programming**

I. Introduction

Backscatter communication is a low-power communication technology for the Internet of things (IoT) and has gained wide popularity recently. Backscatter communication systems have three main components: (a) backscatter transmitters, which are passive tags, (b) a backscatter receiver as the reader, and (c) a radio frequency (RF) carrier emitter source [1]. In monostatic backscatter systems, the reader and RF carrier emitter are embedded in the same device. In backscatter systems, a backscatter device tunes its antenna impedance and communicates with the reader by modulating and reflecting the incident signal from the RF carrier emitter via the reflection coefficient. A portion of the incident carrier signal power is harvested in order to supply the power for the circuit of the backscatter device when it performs backscattering. The remaining portion of the incident signal power is reflected back to the reader by the backscatter device. The reflection coefficients of backscatter devices determine the portion of the incident carrier signal power being reflected back to the reader.

Power-domain non-orthogonal multiple access (NOMA) is an emerging technology for the fifth generation (5G) wireless networks [2]. NOMA can improve the spectral efficiency when compared with orthogonal frequency division multiple access (OFDMA) [3]. With NOMA, signals from multiple users can be multiplexed on the same resource block. By exploiting NOMA technique, the aggregate data rate can be enhanced significantly. In power-domain NOMA, multiple users transmit their messages with different power levels using the same subcarrier. In backscatter systems, the reflection coefficients of backscatter devices are tunable parameters. Signals from multiple backscatter devices can be multiplexed on the same frequency resource block by tunning the reflection coefficient of each device to a different value [4]. Thus, signals from multiple backscatter devices can be separated in the power domain. The reader can decode the signal of each device by exploiting the power difference of the signals.

Backscatter system with NOMA as a multiple access technique has been considered in some recent works. In [4], a hybrid of power-domain NOMA and time division multiple access (TDMA) approach is proposed for a backscatter communication system. In each time slot, signals from multiple backscatter devices located in different spatial regions are multiplexed using NOMA. Simulation results show that backscatter system with NOMA can provide a higher number of successfully decoded bits when compared with a backscatter system using TDMA. In [5], a downlink ambient backscatter NOMA system is proposed. In this system, the backscatter device receives the ambient signal from the base station. Then, it modulates and reflects this signal to the cellular users. The closed form expressions of the outage probabilities are derived in [5]. In [6], an unmanned aerial vehicle (UAV) assisted backscatter system using power-domain NOMA is considered and the throughput of the network is maximized by determining the optimal altitude of the UAV. In [7], a resource allocation problem is formulated for a backscatter system with NOMA and dynamic TDMA. In [8], a cognitive-enabled backscatter network using NOMA is studied and the sum-rate of the backscatter devices is maximized under the multi-slot energy causality constraint. In our previous work [9], we

Manuscript received on Jan. 22, 2021; revised on Jun. 2, 2021 and Sept. 17, 2021; accepted on Jan. 18, 2022. This paper has been published in part in the *Proceedings of IEEE Wireless Communications and Networking Conference (WCNC)*, virtual conference, May 2020. The editor coordinating the review of this paper and approving it for publication was Ming Li.

F. Dashti Ardakani, R. Huang, and V. W.S. Wong are with the Department of Electrical and Computer Engineering, The University of British Columbia, Vancouver, BC, V6T 1Z4, Canada (e-mail: {dashti, ruihuang, vincentw}@ece.ubc.ca).

Color versions of one or more of the figures in this paper are available online at http://ieeexplore.ieee.org.

consider a backscatter system with multicarrier (MC) NOMA. The aggregate data rate of the system is maximized by jointly optimizing the reflection coefficients and subcarrier allocation to the backscatter devices.

Most of the existing works on resource allocation for NOMA backscatter systems focus on improving the aggregate data rate of the system. However, for those backscatter systems supporting IoT applications with low data rate and relaxed latency requirements, optimizing the energy efficiency is crucial. Moreover, the carrier emitter in a backscatter system can be a battery-powered mobile device. In this case, it is beneficial to take the power consumption into account since it can prolong the life cycle of the backscatter NOMA systems. In addition, the energy efficiency depends on both the aggregate data rate and the average power consumption. By maximizing the energy efficiency of the considered system, we can study the tradeoff between optimizing the aggregate throughput and the power consumption.

There are some existing studies on improving the energy efficiency of backscatter systems. An energy-efficient resource allocation scheme is proposed in [10] to determine the optimal time allocation, reflection coefficient, and the transmit power of the carrier emitter in a wireless-powered bistatic backscatter communication system. In [11], the energy efficiency maximization problem is formulated in a UAV-assisted backscatter communication system by optimizing the location of the UAV. In [12], a max-min energy efficiency resource allocation problem is formulated for a wireless powered backscatter network. An iterative algorithm is proposed based on Lagrange dual decomposition. In [13], the energy efficiency of RF powered backscatter networks with harvest-then-transfer protocol is studied. The aforementioned works focus on the energy efficiency of backscatter systems with orthogonal multiple access (OMA) and do not consider NOMA.

The energy efficiency maximization problem for NOMA and energy harvesting networks has been studied in [14]–[17]. In [14], the energy efficiency of a NOMA-enabled backscatter system is maximized by jointly optimizing the allocated power to the NOMA users and the reflection coefficient of the backscatter device. However, the authors in [14] only considered a system with two users, while the device pairing problem in a NOMA backscatter system with multiple users has not been investigated. In addition, the minimum power required for the circuit of the device has not been considered in [14]. The minimum power requirement is crucial to batteryless backscatter devices since they operate solely based on the power of the incident signal.

In [15], the energy efficiency of energy harvesting enabled multi-cell networks with NOMA is studied. The authors formulated an energy efficiency maximization problem, which is nonconvex, and proposed path-following algorithms to solve the problem. In [16], the energy efficiency is maximized in a simultaneous wireless information and power transfer (SWIPT)-based heterogeneous network with NOMA by jointly optimizing the subchannel and transmit power allocation. The device pairing and subchannel allocation problems were solved using heuristic algorithms, i.e., random pairing in [15] and greedy matching in [16]. However, the aforementioned heuristic algorithms cannot jointly optimize the device pairing with the other control variables, such as transmit power and reflection coefficient in the NOMA backscatter systems, in an alternating optimization process. This is because the aforementioned heuristic algorithms do not offer a theoretical guarantee that the objective can be improved monotonically by the algorithm after each iteration, which may affect the overall convergence of the alternating optimization based algorithm.

Apart from the aforementioned heuristic algorithms, the authors in [17] addressed the joint optimization of subchannel allocation and power control in NOMA systems using a search-based approach. The authors in [17] transformed the joint problem using the Lagrangian dual decomposition method. The subchannel allocation problem is solved by allocating each of the subchannels to the small cell that results in the maximum utility. Compared with the heuristic algorithms used in [15] and [16], the algorithm proposed in [17] can jointly optimize the subchannel allocation and transmit power. However, using the search-based method proposed in [17] to determine the device pairing in the NOMA backscatter systems will incur a quadratic time complexity in each iteration. This computational complexity can become higher after we take the necessary matrix operations for determining the utility for each device pairing into account.

In this paper, we study the average energy efficiency optimization of a backscatter system using NOMA as a multiple access technique. In particular, we consider a backscatter system with NOMA, where signals from at most two backscatter devices are multiplexed on the same frequency subcarrier using NOMA in each time slot. We develop an algorithm to maximize the average energy efficiency of the system subject to the minimum circuit power and the minimum data rate requirements of the backscatter devices, and the transmit power constraint of the reader. The main contributions of our work are as follows:

- We formulate the average energy efficiency maximization problem for a backscatter system with NOMA by jointly optimizing the transmit power of the reader, reflection coefficients, and backscatter device pairing coefficients which are binary variables. We guarantee that both the minimum circuit power and data rate requirements of the backscatter devices are satisfied.
- Since the formulated problem is a nonconvex problem with ratio form, we propose an algorithm based on alternating optimization technique to obtain a suboptimal solution for the average energy efficiency maximization problem. We decompose the problem into two different subproblems with objective function in ratio form. We use concave-convex fractional programming and Dinkelbach's algorithm to solve the first subproblem. To solve the second subproblem, we use successive convex approximation (SCA) and difference of convex programming in each iteration of the Dinkelbach's algorithm. The optimization variables are updated iteratively and alternatively until a suboptimal solution is obtained.
- Simulation results show that our proposed algorithm converges in less than 10 iterations to a suboptimal

solution. Our proposed scheme achieves an average energy efficiency that is within 84% of the optimal value. Runtime comparison shows that the runtime of our proposed scheme is less than that of the optimal scheme. The proposed scheme also increases the average energy efficiency of the backscatter system by 7%, 19%, 30%, 93%, and 98% when compared with the genetic algorithm, fixed device pairing scheme, conventional device pairing scheme, maximum transmit power allocation scheme, and random reflection coefficient selection scheme, respectively.
- We also study the problem of maximizing the spectral efficiency of NOMA backscatter system subject to the single-slot and multi-slot energy causality constraints. Simulation results show that NOMA backscatter system achieves a spectral efficiency which is 65% higher than that of backscatter system with OMA scheme. It is also shown that multi-slot energy causality increases the spectral efficiency by 21% when compared with single-slot energy causality.

The rest of this paper is organized as follows. In Section II, we describe the system model and present the average energy efficiency maximization problem. In Section III, we propose an algorithm to solve the formulated problem. The spectral efficiency problem is presented at the end of this section. Performance evaluation and comparisons are presented in Section IV. Conclusion is given in Section V.

In this paper, we use boldface lower case letters to denote vectors. $\mathbf{a}^T$ is used to denote the transpose of vector $\mathbf{a}$; $\mathbb{R}_+$ denotes the set of non-negative real numbers; $\mathbb{R}^N$ denotes the set of all N dimensional vectors with real entries; $\mathbb{R}_+^N$ denotes the non-negative subset of $\mathbb{R}^N$; $\mathbf{a} \preccurlyeq \mathbf{b}$ indicates that vector $\mathbf{a}$ is component-wise smaller than or equal to vector $\mathbf{b}$. We denote the circularly symmetric complex Gaussian distribution with mean γ and variance σ^2 by $\mathcal{CN}(\gamma, \sigma^2)$; $\sim$ stands for "distributed as"; $|.|$ denotes the absolute value of a complex number; $\mathcal{O}(.)$ is used to show the order of complexity of the proposed algorithms.

II. System Model and Problem Formulation

In this paper, we focus on a backscatter communication system with NOMA. As shown in Fig. 1, the system consists of a reader and K single-antenna backscatter devices or passive tags. The reader is equipped with successive interference cancellation (SIC) receiver. Without loss of generality, we consider the allocation of one frequency resource block. For medium access control, we consider a superframe structure. Each superframe is divided into T consecutive time slots. Signals from at most two backscatter devices are multiplexed on the same frequency resource block using NOMA in each time slot. While increasing the number of devices to share the same resource block may improve the spectral efficiency, this also increases the co-channel interference and complexity of decoding the received signal at the reader [18], [19]. In addition, the SIC decoder may suffer from the error propagation and residual cancellation error issues [20, Chap. 6]. When letting more devices share the same

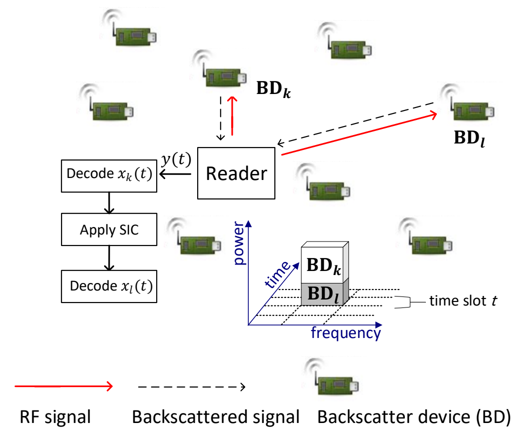

Fig. 1. A backscatter system using NOMA. Signals from two backscatter devices k and l, where $k, l \in \mathcal{K}$, are multiplexed on the same frequency resource block using NOMA in each time slot $t \in \mathcal{T}$. The reader is equipped with an SIC receiver.

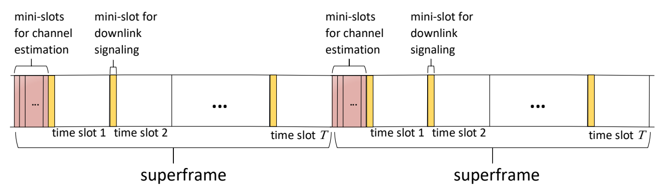

Fig. 2. Structure of two consecutive superframes. Each superframe contains T time slots for energy harvesting and backscattering. Multiple mini-slots are used for channel estimation by the reader. Each time slot also includes one mini-slot for downlink signaling between the reader and backscatter devices.

resource block, the signals that are decoded later in the SIC process may have a lower signal-to-interference-plus-noise ratio (SINR) and hence may not be decoded correctly. This can deteriorate both the energy efficiency and spectral efficiency of the system. Thus, due to the aforementioned implementation issues at the SIC decoder, we assume that only two backscatter devices can share the same resource block.

Let $\mathcal{K} = \{1, \dots, K\}$ denote the set of backscatter devices. Let $\mathcal{T} = \{1, \dots, T\}$ denote the set of time slots in a superframe. In each time slot $t \in \mathcal{T}$, the reader transmits a continuous wave signal as the carrier signal. The backscatter device $k \in \mathcal{K}$ tunes its antenna impedance to switch to a reflection coefficient. Then, the backscatter device harvests energy from the carrier signal to supply the circuit power, and also communicates with the reader by modulating and reflecting the incident carrier signal [21], [22]. The reader decodes the signal of each backscatter device using SIC. We assume that all backscatter devices have data to transmit. The backscatter devices perform delay-tolerant tasks with relaxed latency requirements.

Fig. 2 shows the structure of two consecutive superframes. In the beginning of each superframe, several mini-slots are used for channel estimation by the reader to obtain the channel state information for all the links. The reader needs to send pilot symbols to the backscatter devices and then estimates the channel gain by using least square and linear minimum mean square error techniques [23], [24]. We consider that each superframe contains T time slots for energy harvesting and backscattering. In each time slot, the reader invokes

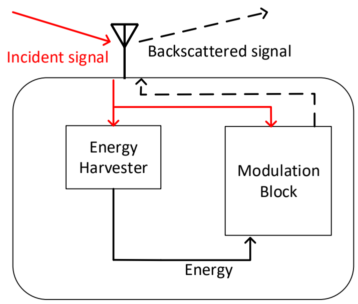

Fig. 3. The architecture of a backscatter transmitter in a passive tag. It consists of an energy harvester and a modulation block. When the backscatter device is modulating and backscattering the incident signal, the energy required for the circuit of the device is obtained from the harvested energy.

an optimization algorithm to determine the control variables including the transmit power, reflection coefficients, and backscatter device pairing. The reader informs the devices about the decisions by downlink signaling in the beginning of each time slot as shown in Fig. 2. After energy harvesting, the incident signal is modulated and reflected back to the reader by the backscatter devices. Each backscatter device transmits its information in one time slot in each superframe. We note that, the system model that we considered in this paper is different from the conventional radio-frequency identification (RFID) systems. In the conventional RFID systems, the RFID tags use random access protocols, such as slotted ALOHA, to perform data transmission. Due to the lack of centralized scheduling, the RFID reader might need to perform bit-level correlation continuously for preamble detection since the reader does not know when the device is transmitting its data. In the considered NOMA backscatter system, a backscatter device can transmit in a particular time slot only if it is scheduled by the centralized controller to do so. Hence, the reader is not required to perform bit-level correlation continuously in the considered system [1].

We consider a flat fading channel model in our system. Let h_k denote the channel gain between the reader and backscatter device $k \in \mathcal{K}$. The channel gain is characterized by both path loss and small-scale fading. We have $h_k = \sqrt{r_k^{-\alpha}} d_k$, where r_k is the distance between the reader and backscatter device k, α is the path loss exponent, and $d_k \sim \mathcal{CN}(0,1)$ is the small-scale fading factor. By estimating the channel at the beginning of each superframe, the global channel state information for all links in the system is available in the reader.

The architecture of a backscatter transmitter is shown in Fig. 3. The backscatter transmitter consists of an energy harvester and a modulation block. The energy harvester harvests a portion of the energy of the incident carrier signal. Similar to [7] and [12], we assume that backscatter devices are not equipped with dedicated power source or battery. Single-slot energy causality is considered for the backscatter devices such that the energy harvested in each time slot can only be used in the current time slot. When the backscatter device is modulating and reflecting the incident carrier signal, the energy required for the circuit of the device is obtained from the harvested energy. The energy harvesting for the circuit operation of the device and the reflection of the incident signal are performed at the same time. Let $P(t)$ denote the power of the carrier signal emitted from the reader in time slot $t \in \mathcal{T}$. Thus, the power of the incident signal at device k in time slot t, which is denoted by $P_k^{\mathrm{I}}(t)$, is equal to $P(t)|h_k|^2$, for $k \in \mathcal{K}, t \in \mathcal{T}$.

We denote the magnitude of the reflection coefficient of device k in time slot t as $\eta_k(t)$, where $0 \leq \eta_k(t) \leq 1$. A portion of $P_k^{\mathrm{I}}(t)$ will be harvested by the energy harvester and will provide the circuit power of device k in time slot t. This portion of power is given by [25]:

$$\begin{aligned} P_k^{\mathrm{H}}(t) &= \rho(1-\eta_k(t))P_k^{\mathrm{I}}(t) \\ &= \rho(1-\eta_k(t))P(t)|h_k|^2, \quad k \in \mathcal{K}, t \in \mathcal{T}, \end{aligned} \tag{1}$$

where ρ denotes the energy harvester efficiency and is between zero and one [26], [27]. This portion of power is utilized by the backscatter device to modulate and reflect the incident carrier signal. The remaining portion of the incident signal power, which is denoted as $P_k^x(t)$, is used for signal transmission of device k in time slot t. We have

$$\begin{aligned} P_k^x(t) &= \eta_k(t)P_k^{\mathrm{I}}(t) \\ &= \eta_k(t)P(t)|h_k|^2, \; k \in \mathcal{K}, t \in \mathcal{T}. \end{aligned} \tag{2}$$

Let $\xi_k(t)$ denote the information symbol of backscatter device k in time slot t with unit average power. Let $x_k(t)$ denote the reflected signal from backscatter device k in time slot t. We have

$$x_k(t) = \sqrt{\eta_k(t)P(t)} h_k \xi_k(t), \quad k \in \mathcal{K}, t \in \mathcal{T}. \tag{3}$$

Consider that two backscatter devices k and l, where $k, l \in \mathcal{K}$, are paired using NOMA in time slot $t \in \mathcal{T}$. The baseband form of received signal in time slot t is as follows:

$$\begin{aligned} y(t) &= h_k x_k(t) + h_l x_l(t) + n(t) \\ &= \sqrt{\eta_k(t)P(t)}(h_k)^2 \xi_k(t) + \sqrt{\eta_l(t)P(t)}(h_l)^2 \xi_l(t) \\ &\quad + n(t), \end{aligned} \tag{4}$$

where $n(t) \sim \mathcal{CN}(0, \sigma^2)$ denotes the circularly symmetric complex Gaussian noise in time slot t in the reader. For backscatter devices k and l operating in time slot t, consider that backscatter device k experiences a better channel gain than backscatter device l, i.e., $|h_k| > |h_l|$. Thus, the reader first decodes the signal of backscatter device k, removes the signal by SIC, and then decodes the signal of backscatter device l. Let binary variable $s_{k,l}(t) \in \{0,1\}$ denote the backscatter device pairing coefficient for backscatter devices k and l in time slot t. The binary variable $s_{k,l}(t)$ is equal to 1 when (a) the backscatter devices k and l are selected to perform NOMA in time slot t, and (b) backscatter device k has a better channel condition and its signal is decoded first in the reader. Otherwise, $s_{k,l}(t)$ is equal to 0. The total power consumption in time slot t consists of the power consumed by the circuit of the backscatter devices in backscatter mode [13]. The power required for the circuit operation is supplied by the harvested power from the carrier signal.

From (1) we can obtain the power consumption of backscatter devices k and l in time slot t by the sum of the harvested powers as follows:

$$\begin{aligned}P_{k,l}(t) &= P_k^{\mathrm{H}}(t) + P_l^{\mathrm{H}}(t) \\ &= \rho(1-\eta_k(t))P(t)|h_k|^2 + \rho(1-\eta_l(t))P(t)|h_l|^2 \\ &= \rho P(t)\left((1-\eta_k(t))|h_k|^2 + (1-\eta_l(t))|h_l|^2\right). \quad (5)\end{aligned}$$

We note that at most two backscatter devices are paired in each time slot. Thus, the total power consumption in time slot t is as follows:

$$\begin{aligned}P^{\mathrm{c}}(t) = \rho P(t) \sum_{k\in\mathcal{K}} \sum_{l\in\mathcal{K}\setminus\{k\}} s_{k,l}(t)\left((1-\eta_k(t))|h_k|^2\right. \\ \left. + \ (1-\eta_l(t))|h_l|^2\right). \quad (6)\end{aligned}$$

The aggregate data rate of backscatter devices k and l in time slot t is given by

$$\begin{aligned}R_{k,l}(t) = \log_2\left(1 + \frac{\eta_k(t)P(t)|h_k|^4}{\eta_l(t)P(t)|h_l|^4 + \sigma^2}\right) \\ + \ \log_2\left(1 + \frac{\eta_l(t)P(t)|h_l|^4}{\sigma^2}\right). \quad (7)\end{aligned}$$

We define $g_k = \frac{|h_k|^4}{\sigma^2}$ and rewrite (7) as follows:

$$\begin{aligned}R_{k,l}(t) = \log_2\left(1 + \frac{\eta_k(t)P(t)g_k}{1+\eta_l(t)P(t)g_l}\right) \\ + \ \log_2\left(1 + \eta_l(t)P(t)g_l\right). \quad (8)\end{aligned}$$

By considering the backscatter device pairing coefficients, the aggregate data rate in time slot t is as follows:

$$\begin{aligned}R(t) = \sum_{k\in\mathcal{K}} \sum_{l\in\mathcal{K}\setminus\{k\}} s_{k,l}(t)\Bigg(\log_2\left(1 + \frac{\eta_k(t)P(t)g_k}{1+\eta_l(t)P(t)g_l}\right) \\ + \log_2\left(1 + \eta_l(t)P(t)g_l\right)\Bigg). \quad (9)\end{aligned}$$

The energy efficiency in each time slot is defined as the ratio of the aggregate data rate to the amount of consumed power in bits per Hertz per Joule (bits/Hz/J). From (6) and (9), we have

$$\begin{aligned}\mathrm{EE}(t) &= \frac{R(t)}{P^{\mathrm{c}}(t)} \\ &= \frac{\sum_{k=1}^{K}\sum_{\substack{l=1\\ l\neq k}}^{K} s_{k,l}(t)\left(\log_2\left(1+\frac{\eta_k(t)P(t)g_k}{1+\eta_l(t)P(t)g_l}\right)+\log_2(1+\eta_l(t)P(t)g_l)\right)}{\rho P(t)\sum_{k\in\mathcal{K}}\sum_{l\in\mathcal{K}\setminus\{k\}} s_{k,l}(t)\left((1-\eta_k(t))|h_k|^2+(1-\eta_l(t))|h_l|^2\right)}.\end{aligned} \quad (10)$$

Our goal is to maximize the average energy efficiency of the system within a superframe. The average energy efficiency maximization problem in the backscatter system with NOMA is as problem (11) which is shown at the bottom of this page. Constraint (11b) ensures that the transmit power of the reader in time slot t cannot exceed $P_{\max}$, which is the maximum power that the reader can transmit. Constraint (11c) ensures that the magnitude of the reflection coefficients is between zero and one. Constraint (11e) ensures that signals from at most two backscatter devices are multiplexed on the frequency resource block in each time slot. Constraint (11f) ensures that each backscatter device is scheduled for transmission in at most one time slot in each superframe. Constraints (11g) and (11h) guarantee that the power harvested in backscatter devices k and l in time slot t is greater than the minimum power required for the circuit of the backscatter devices, which is denoted as $p_{\min}$. The last two constraints guarantee that the data rate of multiplexing backscatter devices is greater than the minimum data rate requirement, denoted as $R_{\min}$. The formulated joint optimization problem consists of both binary variables (i.e., the device pairing variables) and continuous variables (i.e., the transmit power and reflection coefficients). It is challenging to jointly optimize the binary device pairing with the reflection coefficients and power control. In fact, the device pairing subproblem is an integer programming program. While the exhaustive search can find the optimal device pairing, the computational complexity of

$$\underset{\substack{P(t),\ \eta_k(t),\\ s_{k,l}(t),\ k,l\in\mathcal{K},\ t\in\mathcal{T}}}{\text{maximize}} \quad \frac{1}{T}\sum_{t=1}^{T}\frac{\sum_{k\in\mathcal{K}}\sum_{l\in\mathcal{K}\setminus\{k\}} s_{k,l}(t)\left(\log_2\left(1+\frac{\eta_k(t)P(t)g_k}{1+\eta_l(t)P(t)g_l}\right)+\log_2\left(1+\eta_l(t)P(t)g_l\right)\right)}{\rho P(t)\sum_{k\in\mathcal{K}}\sum_{l\in\mathcal{K}\setminus\{k\}} s_{k,l}(t)\left((1-\eta_k(t))|h_k|^2+(1-\eta_l(t))|h_l|^2\right)} \quad (11a)$$

$$\text{subject to} \quad 0 \le P(t) \le P_{\max},\ t\in\mathcal{T} \quad (11b)$$

$$0 \le \eta_k(t) \le 1,\ k\in\mathcal{K},\ t\in\mathcal{T} \quad (11c)$$

$$s_{k,l}(t) \in \{0,1\},\ k,l\in\mathcal{K},\ t\in\mathcal{T} \quad (11d)$$

$$\sum_{k\in\mathcal{K}}\sum_{l\in\mathcal{K}\setminus\{k\}} s_{k,l}(t) \le 1,\ t\in\mathcal{T} \quad (11e)$$

$$\sum_{t\in\mathcal{T}}\sum_{l\in\mathcal{K}\setminus\{k\}} s_{k,l}(t) + \sum_{t'\in\mathcal{T}}\sum_{l'\in\mathcal{K}\setminus\{k\}} s_{l',k}(t') \le 1,\ k\in\mathcal{K} \quad (11f)$$

$$\rho(1-\eta_k(t))P(t)|h_k|^2 \ge s_{k,l}(t)p_{\min},\ k,l\in\mathcal{K},\ t\in\mathcal{T} \quad (11g)$$

$$\rho(1-\eta_l(t))P(t)|h_l|^2 \ge s_{k,l}(t)p_{\min},\ k,l\in\mathcal{K},\ t\in\mathcal{T} \quad (11h)$$

$$\log_2\left(1+\frac{\eta_k(t)P(t)g_k}{1+\eta_l(t)P(t)g_l}\right) \ge s_{k,l}(t)R_{\min},\ k,l\in\mathcal{K},\ t\in\mathcal{T} \quad (11i)$$

$$\log_2\left(1+\eta_l(t)P(t)g_l\right) \ge s_{k,l}(t)R_{\min},\ k,l\in\mathcal{K},\ t\in\mathcal{T}. \quad (11j)$$

this approach is prohibitively high as we need to solve the joint reflection coefficients and power control subproblem for each of the possible device pairing option. Heuristic device pairing algorithms (e.g., random pairing, distance-based pairing) cannot be used as a part of the alternating optimization based algorithm to jointly optimize the device pairing with the reflection coefficients and power control. This is because the heuristic algorithms do not guarantee the convergence to a stationary point of the subproblem, and therefore may affect the convergence of the alternating optimization process. In the next section, we propose an algorithm to solve problem (11) by relaxing the binary device pairing variables into the continuous variables. We also introduce additional constraints such that the solutions obtained from solving the relaxed device pairing subproblem are always in the binary form.

III. Proposed Solution Approach

Problem (11) is a nonconvex optimization problem with an objective function which is in the ratio form. Since all optimization variables and constraints excluding constraint (11f) are independent from one time slot to another time slot, we propose to solve the energy efficiency maximization problem in each time slot separately by optimizing the reflection coefficients, backscatter device pairing, and transmit power of the reader. In other words, we have T separated optimization problems with the objective function in ratio form. In each time slot, the reader optimizes the energy efficiency in the current time slot. To satisfy constraint (11f), we remove the backscatter devices that have been paired in the previous time slots within the superframe. We define the set of backscatter devices in time slot t as follows:

$$\mathcal{K}(t)=\mathcal{K}-\{k,l \mid s_{k,l}(t')=1,\, k,l\in\mathcal{K},\, t'<t\},\; t\in\{2,\dots,T\}, \tag{12}$$

and set $\mathcal{K}(1) = \mathcal{K}$ contains all the backscatter devices in the first time slot. We define vector $\boldsymbol{\eta}(t)$ by concatenating all of the variables $\eta_k(t)$, and also vector $\mathbf{s}(t) \in \mathbb{R}_+^{|\mathcal{K}(t)|^2}$ by concatenating all of the variables $s_{k,l}(t)$, where $|\mathcal{K}(t)|$ is the cardinality of the set $\mathcal{K}(t)$. In time slot $t \in \mathcal{T}$, we solve the following problem:

$$\begin{aligned}
\underset{P(t),\ \boldsymbol{\eta}(t),\ \mathbf{s}(t)}{\text{maximize}}\quad & \frac{U_t(P(t),\boldsymbol{\eta}(t),\mathbf{s}(t))}{F_t(P(t),\boldsymbol{\eta}(t),\mathbf{s}(t))} && \text{(13a)}\\
\text{subject to}\quad & 0 < P(t) \le P_{\max} && \text{(13b)}\\
& 0 \le \eta_k(t) \le 1, \quad k \in \mathcal{K}(t) && \text{(13c)}\\
& s_{k,l}(t) \in \{0,1\}, \quad k,l \in \mathcal{K}(t) && \text{(13d)}\\
& \sum_{k\in\mathcal{K}(t)} \sum_{l\in\mathcal{K}(t), l\neq k} s_{k,l}(t) \le 1 && \text{(13e)}\\
& \rho(1-\eta_k(t))P(t)|h_k|^2 \ge s_{k,l}(t)p_{\min},\, k,l\in\mathcal{K}(t) && \text{(13f)}\\
& \rho(1-\eta_l(t))P(t)|h_l|^2 \ge s_{k,l}(t)p_{\min},\, k,l\in\mathcal{K}(t) && \text{(13g)}\\
& \log_2\left(1+\frac{\eta_k(t)P(t)g_k}{1+\eta_l(t)P(t)g_l}\right) \ge s_{k,l}(t)R_{\min},\quad k,l\in\mathcal{K}(t) && \text{(13h)}\\
& \log_2(1+\eta_l(t)P(t)g_l) \ge s_{k,l}(t)R_{\min},\, k,l\in\mathcal{K}(t), && \text{(13i)}
\end{aligned}$$

where $U_t(P(t),\boldsymbol{\eta}(t),\mathbf{s}(t))$ and $F_t(P(t),\boldsymbol{\eta}(t),\mathbf{s}(t))$ are defined in (14) and (15), as shown at the bottom of this page, respectively. An approach to solve problem (13) is to use alternating optimization technique [28]. We solve the problem separately for $P(t)$ given $s_{k,l}(t), k,l \in \mathcal{K}(t)$ and $\eta_k(t), k \in \mathcal{K}(t)$, and vice versa. First, we optimize the energy efficiency in time slot t with respect to $P(t)$ given the reflection coefficients and backscatter device pairing coefficients. Then, we solve the optimization problem with respect to the reflection coefficients and backscatter device pairing coefficients given the transmit power of the reader. By repeating the above in an iterative manner, we can determine a suboptimal solution in time slot t.

A. Energy Efficiency Maximization with Respect to the Transmit Power of the Reader

Given the reflection coefficients and backscatter device pairing in time slot t, we have the following optimization subproblem:

$$\begin{aligned}
\underset{P(t)}{\text{maximize}}\quad & \frac{U_t(P(t),\boldsymbol{\eta}(t),\mathbf{s}(t))}{F_t(P(t),\boldsymbol{\eta}(t),\mathbf{s}(t))} && \text{(16a)}\\
\text{subject to}\quad & P(t) \ge \frac{s_{k,l}(t)p_{\min}}{\rho(1-\eta_k(t))|h_k|^2}, \quad k,l\in\mathcal{K}(t) && \text{(16b)}\\
& P(t) \ge \frac{s_{k,l}(t)p_{\min}}{\rho(1-\eta_l(t))|h_l|^2}, \quad k,l\in\mathcal{K}(t) && \text{(16c)}\\
& P(t) \ge \frac{s_{k,l}(t)\gamma}{\eta_k(t)g_k-\gamma\eta_l(t)g_l}, \quad k,l\in\mathcal{K}(t) && \text{(16d)}\\
& P(t) \ge \frac{s_{k,l}(t)\gamma}{\eta_l(t)g_l}, \quad k,l\in\mathcal{K}(t) && \text{(16e)}\\
& \text{constraint (13b)},
\end{aligned}$$

where $\gamma = 2^{R_{\min}} - 1$ is the SINR threshold. Appendix A shows the derivation of constraints (16d) and (16e). We define function $f(P(t))$ and constant C_0 as follows:

$$f(P(t))=\sum_{k\in\mathcal{K}(t)}\sum_{\substack{l\in\mathcal{K}(t),\\ l\neq k}} s_{k,l}(t)(\log_2(1+P(t)(\eta_k(t)g_k+\eta_l(t)g_l))), \tag{17}$$

$$U_t(P(t),\boldsymbol{\eta}(t),\mathbf{s}(t)) = \sum_{k\in\mathcal{K}(t)}\sum_{l\in\mathcal{K}(t),l\neq k} s_{k,l}(t)\left(\log_2\left(1+\frac{\eta_k(t)P(t)g_k}{1+\eta_l(t)P(t)g_l}\right)+\log_2\left(1+\eta_l(t)P(t)g_l\right)\right) \tag{14}$$

$$F_t(P(t),\boldsymbol{\eta}(t),\mathbf{s}(t)) = \rho P(t)\sum_{k\in\mathcal{K}(t)}\sum_{l\in\mathcal{K}(t),l\neq k} s_{k,l}(t)\left((1-\eta_k(t))|h_k|^2+(1-\eta_l(t))|h_l|^2\right) \tag{15}$$

Algorithm 1: Dinkelbach's Algorithm for the First Subproblem: Problem (19)

Initialize $\lambda_1^{(1)} := 0$.
Set iteration index $n := 1$ and $\delta_1 \ll 1$.
repeat
  Given $\lambda_1^{(n)}$, solve problem (21) to obtain $P^{(n)}(t)$.
  $\lambda_1^{(n+1)} := \frac{f\left(P^{(n)}(t)\right)}{C_0 P^{(n)}(t)}$.
  $n := n + 1$.
until $f\left(P^{(n-1)}(t)\right) - \lambda_1^{(n)} C_0 P^{(n-1)}(t) \leq \delta_1$;

$$C_0 = \rho \sum_{k \in \mathcal{K}(t)} \sum_{\substack{l \in \mathcal{K}(t), \\ l \neq k}} s_{k,l}(t) \Big(\big(1 - \eta_k(t)\big) |h_k|^2 + \big(1 - \eta_l(t)\big) |h_l|^2 \Big). \tag{18}$$

Thus, we can represent problem (16) in the following form:

$$\begin{aligned} &\underset{P(t)}{\text{maximize}} && \frac{f(P(t))}{C_0 P(t)} && (19a) \\ &\text{subject to} && P_{\text{min}}(t) \leq P(t) \leq P_{\text{max}}, && (19b) \end{aligned}$$

where $P_{\text{min}}(t)$ is the lower bound of $P(t)$ and is obtained from constraints (16b)$-$(16e). $P_{\text{min}}(t)$ is defined as follows:

$$P_{\text{min}}(t) = \max_{k,l \in \mathcal{K}(t)} \left\{ \frac{s_{k,l}(t) p_{\text{min}}}{\rho(1 - \eta_k(t))|h_k|^2}, \frac{s_{k,l}(t) p_{\text{min}}}{\rho(1 - \eta_l(t))|h_l|^2}, \frac{s_{k,l}(t)\gamma}{\eta_k(t) g_k - \gamma \eta_l(t) g_l}, \frac{s_{k,l}(t)\gamma}{\eta_l(t) g_l} \right\}. \tag{20}$$

We note that in the objective function (16a), only one term in the summations in the numerator and denominator is nonzero. Thus, problem (16) (or the equivalent problem (19)) has the form of single-ratio fractional programming [29]–[32]. Specifically, function $f(P(t))$ is in logarithmic form and is concave with respect to $P(t)$. The denominator of the objective function in (19) is an affine function of $P(t)$. The feasible set is also convex. Thus, problem (19) is a concave-convex fractional programming problem. We can use techniques such as Dinkelbach's algorithm to solve this subproblem [33]. By using Dinkelbach's algorithm, problem (19) is equivalent to:

$$\begin{aligned} &\underset{P(t),\ \lambda_1}{\text{maximize}} && Q(P(t), \lambda_1) && (21a) \\ &\text{subject to} && \lambda_1 \geq 0, && (21b) \\ & && \text{constraint (19b)}, && \end{aligned}$$

where $Q(P(t), \lambda_1) = f(P(t)) - \lambda_1 C_0 P(t)$ is the objective function and λ_1 is an auxiliary variable. Problem (21) can be solved in an iterative manner. Given λ_1, problem (21) is a convex optimization problem. It can be solved by standard optimization tools such as CVX [34]. The algorithm for solving this problem is summarized in Algorithm 1. In this algorithm, we first set λ_1 to zero. In each iteration of the algorithm, we solve problem (21) to find the optimal transmit power of the reader in time slot t. Then, we update the value of λ_1. We repeat the process until the value of the objective function (21a) is less than a threshold, denoted as δ_1.

B. Energy Efficiency Maximization with Respect to the Reflection Coefficients and Backscatter Device Pairing Coefficients

For the second subproblem, given the transmit power of the reader $P(t)$, we have the following optimization problem:

$$\begin{aligned} &\underset{\boldsymbol{\eta}(t),\ \mathbf{s}(t)}{\text{maximize}} && \frac{U_t(P(t), \boldsymbol{\eta}(t), \mathbf{s}(t))}{F_t(P(t), \boldsymbol{\eta}(t), \mathbf{s}(t))} && (22) \\ &\text{subject to} && \text{constraints (13c)}-\text{(13i)}. && \end{aligned}$$

The objective function of problem (22) is in ratio form. Since only one term of the summations in the numerator and denominator is nonzero, this problem is a single-ratio fractional programming problem. Using Dinkelbach's algorithm for this subproblem, we decouple the numerator and denominator of the objective function. The equivalent form of problem (22) is as follows:

$$\begin{aligned} \underset{\lambda_2,\ \boldsymbol{\eta}(t),\ \mathbf{s}(t)}{\text{maximize}} & \sum_{k \in \mathcal{K}(t)} \sum_{\substack{l \in \mathcal{K}(t), \\ l \neq k}} s_{k,l}(t) \Big(\log_2 \big(1 + P(t) \big(\eta_k(t) g_k + \eta_l(t) g_l \big) \big) \Big) \\ & - \lambda_2 \rho P(t) \sum_{k \in \mathcal{K}(t)} \sum_{\substack{l \in \mathcal{K}(t), \\ l \neq k}} s_{k,l}(t) \Big(\big(1 - \eta_k(t)\big) |h_k|^2 + \big(1 - \eta_l(t)\big) |h_l|^2 \Big) \end{aligned} \tag{23a}$$

$$\begin{aligned} &\text{subject to} && \lambda_2 \geq 0, && (23b) \\ & && \text{constraints (13c)}-\text{(13i)}. && \end{aligned}$$

Appendix B shows how we obtain the first term of (23a). The objective function in (23a) is nonconvex due to the multiplication between the reflection coefficients $\eta_k(t)$ and backscatter device pairing coefficients $s_{k,l}(t)$. To tackle this problem, we define variables $\tilde{\eta}_{k,l,k}(t) = s_{k,l}(t)\eta_k(t)$ and $\tilde{\eta}_{k,l,l}(t) = s_{k,l}(t)\eta_l(t)$. We define vector $\tilde{\boldsymbol{\eta}}(t) \in \mathbb{R}_+^{2|\mathcal{K}(t)|^2}$ by concatenating all of the variables $\tilde{\eta}_{k,l,k}(t)$ and $\tilde{\eta}_{k,l,l}(t)$. Furthermore, we note that constraint (13d) is nonconvex. We can rewrite this constraint as follows:

$$0 \leq s_{k,l}(t) \leq 1, \qquad k, l \in \mathcal{K}(t) \tag{24a}$$

$$s_{k,l}(t) - (s_{k,l}(t))^2 \leq 0, \qquad k, l \in \mathcal{K}(t). \tag{24b}$$

Constraint (24b) is nonconvex. This constraint is considered as difference of convex functions [18]. Since function $(s_{k,l}(t))^2$ is differentiable, we can use the first-order condition for convex functions to approximate $(s_{k,l}(t))^2$ by an affine function. Consider i as an iteration index starting from one. For any given $s_{k,l}^{(i)}(t)$, we have

$$(s_{k,l}(t))^2 \geq (s_{k,l}^{(i)}(t))^2 + 2 s_{k,l}^{(i)}(t)(s_{k,l}(t) - s_{k,l}^{(i)}(t)), k, l \in \mathcal{K}(t). \tag{25}$$

Thus, given $s_{k,l}^{(i)}(t)$, constraint (24b) can be written as follows:

$$s_{k,l}(t) - (s_{k,l}^{(i)}(t))^2 - 2 s_{k,l}^{(i)}(t)(s_{k,l}(t) - s_{k,l}^{(i)}(t)) \leq 0, k, l \in \mathcal{K}(t). \tag{26}$$

Note that the variable $\tilde{\eta}_{k,l,k}(t) = s_{k,l}(t)\eta_k(t)$ is the product of two variables. To decompose the product terms, we introduce the following additional constraints to our problem [18]:

$$\tilde{\eta}_{k,l,k}(t) \leq s_{k,l}(t), \qquad k, l \in \mathcal{K}(t) \tag{27a}$$

$$\tilde{\eta}_{k,l,k}(t) \leq \eta_k(t), \qquad k, l \in \mathcal{K}(t) \tag{27b}$$

$$\tilde{\eta}_{k,l,k}(t) \geq \eta_k(t) - (1 - s_{k,l}(t)), \quad k, l \in \mathcal{K}(t) \tag{27c}$$

$$\tilde{\eta}_{k,l,k}(t) \geq 0, \quad k, l \in \mathcal{K}(t). \tag{27d}$$

Since $s_{k,l}(t)$ is a binary variable, i.e., $s_{k,l}(t) \in \{0, 1\}$, we can rewrite constraint (13h) as follows:

$$\log_2\left(1 + \frac{s_{k,l}(t)\eta_k(t)P(t)g_k}{1 + s_{k,l}(t)\eta_l(t)P(t)g_l}\right) \geq s_{k,l}(t)R_{\min}, k, l \in \mathcal{K}(t),$$

$$\log_2\left(\frac{1 + s_{k,l}(t)\eta_k(t)P(t)g_k + s_{k,l}(t)\eta_l(t)P(t)g_l}{1 + s_{k,l}(t)\eta_l(t)P(t)g_l}\right) \geq s_{k,l}(t)R_{\min}, k, l \in \mathcal{K}(t). \tag{28}$$

Using auxiliary variables $\tilde{\eta}_{k,l,k}(t)$ and $\tilde{\eta}_{k,l,l}(t)$, we have

$$\log_2\left(\frac{1 + P(t)(\tilde{\eta}_{k,l,k}(t)g_k + \tilde{\eta}_{k,l,l}(t)g_l)}{1 + \tilde{\eta}_{k,l,l}(t)P(t)g_l}\right) \geq s_{k,l}(t)R_{\min}, k, l \in \mathcal{K}(t),$$

$$\log_2\left(1 + P(t)(\tilde{\eta}_{k,l,k}(t)g_k + \tilde{\eta}_{k,l,l}(t)g_l)\right) - \log_2\left(1 + \tilde{\eta}_{k,l,l}(t)P(t)g_l\right) \geq s_{k,l}(t)R_{\min}, k, l \in \mathcal{K}(t). \tag{29}$$

Constraint (29) is the difference of two concave functions and is a nonconvex constraint. Note that the function $\log_2(1 + \tilde{\eta}_{k,l,l}(t)P(t)g_l)$ is a differentiable concave function. Thus, we can use the first-order condition for concave functions and approximate it by an affine function [35]. Consider i as an iteration index starting from one. For any given $\tilde{\eta}_{k,l,l}^{(i)}(t)$, we have

$$\log_2\left(1 + \tilde{\eta}_{k,l,l}(t)P(t)g_l\right) \leq \log_2\left(1 + \tilde{\eta}_{k,l,l}^{(i)}(t)P(t)g_l\right) + \frac{P(t)g_l(\tilde{\eta}_{k,l,l}(t) - \tilde{\eta}_{k,l,l}^{(i)}(t))}{1 + \tilde{\eta}_{k,l,l}^{(i)}(t)P(t)g_l}, \ k, l \in \mathcal{K}(t). \tag{30}$$

According to inequality (30), we have the following inequality:

$$\begin{aligned}
&\log_2\left(1 + P(t)(\tilde{\eta}_{k,l,k}(t)g_k + \tilde{\eta}_{k,l,l}(t)g_l)\right) - \log_2\left(1 + \tilde{\eta}_{k,l,l}(t)P(t)g_l\right) \\
&\geq \log_2\left(1 + P(t)(\tilde{\eta}_{k,l,k}(t)g_k + \tilde{\eta}_{k,l,l}(t)g_l)\right) - \log_2\left(1 + \tilde{\eta}_{k,l,l}^{(i)}(t)P(t)g_l\right) - \frac{P(t)g_l(\tilde{\eta}_{k,l,l}(t) - \tilde{\eta}_{k,l,l}^{(i)}(t))}{1 + \tilde{\eta}_{k,l,l}^{(i)}(t)P(t)g_l}, \\
&\qquad k, l \in \mathcal{K}(t).
\end{aligned} \tag{31}$$

Thus, we can replace function $\log_2(1 + \tilde{\eta}_{k,l,l}(t)P(t)g_l)$ in the left hand side of (29) by the right hand side of (30) and rewrite constraint (29) as follows:

$$\log_2\left(1 + P(t)(\tilde{\eta}_{k,l,k}(t)g_k + \tilde{\eta}_{k,l,l}(t)g_l)\right) - \log_2\left(1 + \tilde{\eta}_{k,l,l}^{(i)}(t)P(t)g_l\right) - \frac{P(t)g_l(\tilde{\eta}_{k,l,l}(t) - \tilde{\eta}_{k,l,l}^{(i)}(t))}{1 + \tilde{\eta}_{k,l,l}^{(i)}(t)P(t)g_l} \geq s_{k,l}(t)R_{\min}, k, l \in \mathcal{K}(t). \tag{32}$$

We can guarantee that the solutions that satisfy constraint (32) are feasible solutions to the original problem. This is because according to (31), if constraint (32) is satisfied, constraint (29) is also satisfied. We also rewrite constraint (13i) as follows:

$$\log_2\left(1 + \tilde{\eta}_{k,l,l}(t)P(t)g_l\right) \geq s_{k,l}(t)R_{\min}, \ k, l \in \mathcal{K}(t). \tag{33}$$

Since $s_{k,l}(t)$ is a binary variable, i.e., $s_{k,l}(t) \in \{0, 1\}$, we can rewrite the first term of (23a) as follows:

$$\begin{aligned}
&\sum_{k \in \mathcal{K}(t)} \sum_{\substack{l \in \mathcal{K}(t) \\ l \neq k}} \log_2\left(1 + s_{k,l}(t)P(t)(\eta_k(t)g_k + \eta_l(t)g_l)\right) \\
&= \sum_{k \in \mathcal{K}(t)} \sum_{\substack{l \in \mathcal{K}(t) \\ l \neq k}} \log_2\left(1 + P(t)(s_{k,l}(t)\eta_k(t)g_k + s_{k,l}(t)\eta_l(t)g_l)\right) \\
&= \sum_{k \in \mathcal{K}(t)} \sum_{\substack{l \in \mathcal{K}(t) \\ l \neq k}} \log_2\left(1 + P(t)(\tilde{\eta}_{k,l,k}(t)g_k + \tilde{\eta}_{k,l,l}(t)g_l)\right).
\end{aligned} \tag{34}$$

By including the auxiliary variables and the new constraints, we have the following problem:

$$\begin{aligned}
\underset{\lambda_2, \tilde{\boldsymbol{\eta}}(t), \mathbf{s}(t)}{\text{maximize}} \ & \sum_{k \in \mathcal{K}(t)} \sum_{\substack{l \in \mathcal{K}(t), \\ l \neq k}} \log_2\left(1 + P(t)(\tilde{\eta}_{k,l,k}(t)g_k + \tilde{\eta}_{k,l,l}(t)g_l)\right) \\
& - \lambda_2 \rho P(t) \sum_{k \in \mathcal{K}(t)} \sum_{\substack{l \in \mathcal{K}(t), \\ l \neq k}} (s_{k,l}(t) - \tilde{\eta}_{k,l,k}(t))|h_k|^2 \\
& - \lambda_2 \rho P(t) \sum_{k \in \mathcal{K}(t)} \sum_{\substack{l \in \mathcal{K}(t), \\ l \neq k}} (s_{k,l}(t) - \tilde{\eta}_{k,l,l}(t))|h_l|^2 & (35a) \\
\text{subject to} \ & 0 \leq \tilde{\eta}_{k,l,k}(t) \leq 1, \ k, l \in \mathcal{K}(t) & (35b) \\
& 0 \leq \tilde{\eta}_{k,l,l}(t) \leq 1, \ k, l \in \mathcal{K}(t) & (35c) \\
& \rho(1 - \tilde{\eta}_{k,l,k}(t))P(t)|h_k|^2 \geq s_{k,l}(t)p_{\min}, k, l \in \mathcal{K}(t) & (35d) \\
& \rho(1 - \tilde{\eta}_{k,l,l}(t))P(t)|h_l|^2 \geq s_{k,l}(t)p_{\min}, k, l \in \mathcal{K}(t) & (35e) \\
& \text{constraints (13e), (23b), (24a), (26), (27a)–(27c), (32), (33).}
\end{aligned}$$

We further define functions $A(\mathbf{s}(t), \tilde{\boldsymbol{\eta}}(t))$ and $B(\mathbf{s}(t), \tilde{\boldsymbol{\eta}}(t))$ as follows:

$$A(\mathbf{s}(t), \tilde{\boldsymbol{\eta}}(t)) = \sum_{k \in \mathcal{K}(t)} \sum_{\substack{l \in \mathcal{K}(t), \\ l \neq k}} \log_2\left(1 + P(t)(\tilde{\eta}_{k,l,k}(t)g_k + \tilde{\eta}_{k,l,l}(t)g_l)\right), \tag{36a}$$

$$B(\mathbf{s}(t), \tilde{\boldsymbol{\eta}}(t)) = \rho P(t) \sum_{k \in \mathcal{K}(t)} \sum_{l \in \mathcal{K}(t), l \neq k} (s_{k,l}(t) - \tilde{\eta}_{k,l,k}(t))|h_k|^2 + \rho P(t) \sum_{k \in \mathcal{K}(t)} \sum_{l \in \mathcal{K}(t), l \neq k} (s_{k,l}(t) - \tilde{\eta}_{k,l,l}(t))|h_l|^2. \tag{36b}$$

Problem (35) can be solved in an iterative manner. Given λ_2, this problem is a convex optimization problem. It can be solved using standard optimization tools such as CVX.

The proposed algorithm for solving problem (22) is summarized in Algorithm 2. In each iteration of Dinkelbach's algorithm, given λ_2, we solve problem (35) using SCA to obtain the reflection coefficients and backscatter device pairing coefficients. Then, we update λ_2, and repeat the Dinkelbach's algorithm until the objective function (35a) achieves a value less than a threshold, denoted as δ_2. To improve the performance of SCA method, we repeat the algorithm for multiple number of initializations, i.e., we run SCA for different initial points to obtain a local

Algorithm 2: Iterative Algorithm for the Second Subproblem: Problem (22)

Set $\delta_2 \ll 1$, maximum number of initializations $J_{\max}$, and maximum number of iterations $I_{\max}$.
Set initialization index $j := 1$.
while $j \leq J_{\max}$ **do**
  Initialize $\lambda_2^{(1,j)} := 0$ and set iteration index $n := 1$.
  repeat
    Set iteration index $i := 1$ and set initial points $\mathbf{s}^{(n,j,1)}(t)$ and $\tilde{\boldsymbol{\eta}}^{(n,j,1)}(t)$.
    while $i \leq I_{\max}$ **do**
      Solve problem (35) for given $\lambda_2^{(n,j)}$, $\mathbf{s}^{(n,j,i)}(t)$ and $\tilde{\boldsymbol{\eta}}^{(n,j,i)}(t)$ and store the resulting variables as $\mathbf{s}_{\text{succ}}(t)$ and $\tilde{\boldsymbol{\eta}}_{\text{succ}}(t)$.
      Set $i := i+1$, $\mathbf{s}^{(n,j,i)}(t) := \mathbf{s}_{\text{succ}}(t)$ and $\tilde{\boldsymbol{\eta}}^{(n,j,i)}(t) := \tilde{\boldsymbol{\eta}}_{\text{succ}}(t)$.
    end
    Set $\mathbf{s}_{\text{temp}}^{(n,j)}(t) := \mathbf{s}^{(n,j,i)}(t)$ and $\tilde{\boldsymbol{\eta}}_{\text{temp}}^{(n,j)}(t) := \tilde{\boldsymbol{\eta}}^{(n,j,i)}(t)$.
    $\lambda_2^{(n+1,j)} := \frac{A(\mathbf{s}_{\text{temp}}^{(n,j)}(t), \tilde{\boldsymbol{\eta}}_{\text{temp}}^{(n,j)}(t))}{B(\mathbf{s}_{\text{temp}}^{(n,j)}(t), \tilde{\boldsymbol{\eta}}_{\text{temp}}^{(n,j)}(t))}$.
    $n := n+1$.
  until $A\left(\mathbf{s}_{\text{temp}}^{(n-1,j)}(t), \tilde{\boldsymbol{\eta}}_{\text{temp}}^{(n-1,j)}(t)\right) - \lambda_2^{(n,j)} B\left(\mathbf{s}_{\text{temp}}^{(n-1,j)}(t), \tilde{\boldsymbol{\eta}}_{\text{temp}}^{(n-1,j)}(t)\right) \leq \delta_2$;
  Set $\mathbf{s}_{\text{saved}}^{(j)}(t) := \mathbf{s}_{\text{temp}}^{(n-1,j)}(t)$ and $\tilde{\boldsymbol{\eta}}_{\text{saved}}^{(j)}(t) := \tilde{\boldsymbol{\eta}}_{\text{temp}}^{(n-1,j)}(t)$.
  Set $j := j+1$.
end
$(\mathbf{s}(t), \tilde{\boldsymbol{\eta}}(t)) := \underset{\mathbf{s}_{\text{saved}}^{(j)}(t), \tilde{\boldsymbol{\eta}}_{\text{saved}}^{(j)}(t), j \in \{1,\ldots,J_{\max}\}}{\arg\max} \frac{A(\mathbf{s}_{\text{saved}}^{(j)}(t), \tilde{\boldsymbol{\eta}}_{\text{saved}}^{(j)}(t))}{B(\mathbf{s}_{\text{saved}}^{(j)}(t), \tilde{\boldsymbol{\eta}}_{\text{saved}}^{(j)}(t))}$.
Obtain $\boldsymbol{\eta}(t)$ from $\tilde{\boldsymbol{\eta}}(t)$.

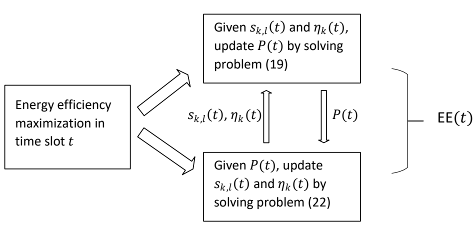

Fig. 4. Alternating optimization algorithm for energy efficiency maximization problem in time slot t.

optimal solution for the reflection coefficients and backscatter device pairing coefficients. Finally, we choose the reflection coefficients and backscatter device pairing coefficients that maximize the energy efficiency. Since we have $\tilde{\eta}_{k,l,k}(t) = s_{k,l}(t)\eta_k(t)$ and $\tilde{\eta}_{k,l,l}(t) = s_{k,l}(t)\eta_l(t)$, we can obtain $\boldsymbol{\eta}(t)$ from vector $\tilde{\boldsymbol{\eta}}(t)$.

To obtain a suboptimal solution for energy efficiency maximization in time slot $t \in \mathcal{T}$, we repeat the algorithms proposed for solving the two separated subproblems. The optimization variables are updated iteratively and alternatively until the difference between the value of energy efficiency in two consecutive iterations is less than a threshold. Fig. 4 shows the alternating optimization algorithm for solving the energy efficiency maximization problem in time slot t. This algorithm is also summarized in Algorithm 3. In each time slot, we update the set of backscatter devices according to (12).

Algorithm 3: Alternating Optimization Algorithm for Energy Efficiency Maximization in Time Slot $t \in \mathcal{T}$

Initialize $P(t), \mathbf{s}(t)$ and $\boldsymbol{\eta}(t)$ and calculate the initial value of energy efficiency in time slot t, $\text{EE}^{(1)}(t)$.
Set iteration index $m := 1$ and $\epsilon \ll 1$.
repeat
  Given $\mathbf{s}(t)$ and $\boldsymbol{\eta}(t)$, update $P(t)$ using Algorithm 1
  Given $P(t)$, update $\mathbf{s}(t)$ and $\boldsymbol{\eta}(t)$ using Algorithm 2.
  Calculate $\text{EE}^{(m+1)}(t)$.
  $m := m+1$.
until $|\text{EE}^{(m)}(t) - \text{EE}^{(m-1)}(t)| \leq \epsilon$;

Then, we use Algorithm 3 to optimize the energy efficiency in the corresponding time slot. By repeating this process for the number of time slots within a superframe, a suboptimal value for the objective function in problem (11) can be obtained.

The value of the objective function of problem (11) cannot increase infinitely due to the constraints on the optimization variables. When Algorithm 3 is invoked, the value of the energy efficiency increases in each iteration m until achieving convergence. The solution achieved by the proposed alternating optimization algorithm may not provide a global optimal solution. This is because problem (11) is not convex with respect to the optimization variables. In addition, solving the second subproblem using SCA gives us a suboptimal solution for the reflection coefficients and backscatter device pairing.

C. Computational Complexity

The computational complexity of alternating optimization algorithm depends on the number of iterations required in Algorithm 3 and the computational complexity of solving each subproblem. In this subsection, we evaluate the worst case complexity of alternating optimization algorithm. Let I_3 denote the number of iterations in Algorithm 3. The optimization of transmit power of the reader, given the reflection coefficients and backscatter device pairing, needs to solve a convex problem in each Dinkelbach's iteration. Suppose I_{sub1} iterations are required. Solving a convex problem has a polynomial time complexity in the number of optimization variables [36]. Considering that the first subproblem has only one variable, the asymptotic computational complexity of this subproblem is as $\mathcal{O}(I_{\text{sub1}})$. For optimization of reflection coefficients and backscatter device pairing, we solve a convex problem with $3K^2$ variables using SCA in each Dinkelbach's iteration. We repeat this algorithm for multiple number of initializations denoted as $J_{\max}$. Thus, the asymptotic complexity of the second subproblem is as $\mathcal{O}\left(J_{\max} I_{\text{sub2}} I_{\max} (3K^2)^z\right)$, where $1 \leq z \leq 4$ [36]. Parameters I_{sub2} and $I_{\max}$ are the number of iterations required for Dinkelbach's algorithm and SCA, respectively. Overall, the asymptotic computational complexity of running Algorithm 3 in one time slot is given by $\mathcal{O}\left(I_3 J_{\max} I_{\text{sub2}} I_{\max} K^{2z} + I_3 I_{\text{sub1}}\right)$. If we consider that $I_{\text{sub1}} \approx I_{\text{sub2}}$, the computational complexity can be approximated by $\mathcal{O}\left(I_3 J_{\max} I_{\text{sub}} I_{\max} K^{2z}\right)$, where I_{sub} is the number of Dinkelbach's iterations required for both subproblems.

D. Spectral Efficiency in the Backscatter System with NOMA

In this subsection, we study the spectral efficiency of the backscatter system with NOMA. Our goal is to maximize the spectral efficiency of the system subject to the minimum circuit power requirements and minimum data rate constraints of the backscatter devices. We consider two different scenarios. In the first scenario, single-slot energy causality constraint is considered for the batteryless backscatter devices such that the energy harvested in each time slot can be used only in the current time slot. In the second scenario, we assume that backscatter devices have battery for energy storage, and the energy harvested in each time slot can be stored for later use [8], [13].

The spectral efficiency of the backscatter system with NOMA over a superframe in bits per second per Hertz (bits/s/Hz) is defined as follows [28]:

$$\begin{aligned} \mathrm{SE} &= \sum_{t\in\mathcal{T}}\sum_{k\in\mathcal{K}}\sum_{l\in\mathcal{K}\setminus\{k\}} R_{k,l}(t) \\ &= \sum_{t\in\mathcal{T}}\sum_{k\in\mathcal{K}}\sum_{l\in\mathcal{K}\setminus\{k\}} s_{k,l}(t)\log_2\left(1+\frac{\eta_k(t)P(t)g_k}{1+\eta_l(t)P(t)g_l}\right) \\ &\quad + \sum_{t\in\mathcal{T}}\sum_{k\in\mathcal{K}}\sum_{l\in\mathcal{K}\setminus\{k\}} s_{k,l}(t)\log_2\left(1+\eta_l(t)P(t)g_l\right). \end{aligned} \tag{37}$$

Considering the single-slot energy causality, we can formulate the spectral efficiency maximization problem by jointly optimizing the reflection coefficients, backscatter device pairing, and transmit power of the reader as follows:

$$\begin{aligned} \underset{\substack{P(t),\ \eta_k(t),\\ s_{k,l}(t),\ k,l\in\mathcal{K},t\in\mathcal{T}}}{\text{maximize}} \quad & \sum_{t=1}^{T}\sum_{k=1}^{K}\sum_{\substack{l=1\\ l\neq k}}^{K} s_{k,l}(t)\log_2\left(1+\frac{\eta_k(t)P(t)g_k}{1+\eta_l(t)P(t)g_l}\right) \\ & + \sum_{t=1}^{T}\sum_{k=1}^{K}\sum_{\substack{l=1\\ l\neq k}}^{K} s_{k,l}(t)\log_2(1+\eta_l(t)P(t)g_l) \\ \text{subject to} \quad & \text{constraints (11b)}-\text{(11j)}. \end{aligned} \tag{38}$$

To solve problem (38), Proposition 1 is provided to obtain the optimal transmit power of the reader in each time slot.

Proposition 1: To maximize the spectral efficiency of NOMA backscatter system, the optimal transmit power of the reader in each time slot is $P_{\max}$.

Proof: Given the reflection coefficients and backscatter device pairing in each time slot, the objective function (38) increases with the increase of $P(t), t\in\mathcal{T}$. Thus, optimal $P^*(t)$ is determined by the upper bound of $P(t)$. We note that the combination of constraints (11g), (11h), (11i), and (11j) gives the lower bound of $P(t)$. The upper bound of $P(t)$ is $P_{\max}$. Thus, we have $P^*(t)=P_{\max}$.

We maximize the spectral efficiency in each time slot separately. Using the variables that we have already defined and considering single-slot energy causality, we can formulate the spectral efficiency maximization problem in time slot t as follows:

$$\underset{\tilde{\boldsymbol{\eta}}(t),\ \mathbf{s}(t)}{\text{maximize}} \sum_{k\in\mathcal{K}(t)}\sum_{\substack{l\in\mathcal{K}(t),\\ l\neq k}} \log_2\!\left(1+P_{\max}(\tilde{\eta}_{k,l,k}(t)g_k+\tilde{\eta}_{k,l,l}(t)g_l)\right) \tag{39a}$$

$$\text{subject to } \rho(1-\tilde{\eta}_{k,l,k}(t))P_{\max}|h_k|^2 \geq s_{k,l}(t)p_{\min},\ k,l\in\mathcal{K}(t) \tag{39b}$$

$$\rho(1-\tilde{\eta}_{k,l,l}(t))P_{\max}|h_l|^2 \geq s_{k,l}(t)p_{\min},\ k,l\in\mathcal{K}(t) \tag{39c}$$

$$\begin{aligned} &\log_2\left(1+P_{\max}(\tilde{\eta}_{k,l,k}(t)g_k+\tilde{\eta}_{k,l,l}(t)g_l)\right) \\ &-\log_2\!\left(1+\tilde{\eta}_{k,l,l}^{(i)}(t)P_{\max}g_l\right) \\ &-\frac{P_{\max}g_l(\tilde{\eta}_{k,l,l}(t)-\tilde{\eta}_{k,l,l}^{(i)}(t))}{1+\tilde{\eta}_{k,l,l}^{(i)}(t)P_{\max}g_l} \geq s_{k,l}(t)R_{\min},\ k,l\in\mathcal{K}(t) \end{aligned} \tag{39d}$$

$$\log_2\left(1+\tilde{\eta}_{k,l,l}P_{\max}g_l\right) \geq s_{k,l}(t)R_{\min},\ k,l\in\mathcal{K}(t). \tag{39e}$$

$$\text{constraints (13e), (24a), (26), (27a)}-\text{(27c), (35b), (35c)}.$$

Algorithm 4: SCA Algorithm for Spectral Efficiency Maximization in Time Slot $t\in\mathcal{T}$

Initialize maximum number of iterations $N_{\max}$, iteration index $i:=1$ and starting points $\mathbf{s}^{(1)}(t)$ and $\tilde{\boldsymbol{\eta}}^{(1)}(t)$.
while $i\leq N_{\max}$ **do**
  Solve problem (39) for given $\mathbf{s}^{(i)}(t)$ and $\tilde{\boldsymbol{\eta}}^{(i)}(t)$ and store the backscatter device pairing and reflection coefficients as $\mathbf{s}(t)$ and $\tilde{\boldsymbol{\eta}}(t)$.
  Set $i:=i+1$, $\mathbf{s}^{(i)}(t):=\mathbf{s}(t)$ and $\tilde{\boldsymbol{\eta}}^{(i)}(t):=\tilde{\boldsymbol{\eta}}(t)$.
end
$\mathbf{s}^*(t):=\mathbf{s}^{(i)}(t)$ and $\tilde{\boldsymbol{\eta}}^*(t):=\tilde{\boldsymbol{\eta}}^{(i)}(t)$.

Problem (39) is a convex problem. We use SCA in an iterative algorithm to solve this problem. The algorithm for solving this problem is summarized in Algorithm 4. In the case that multi-slot energy causality is considered, the constraints related to the minimum circuit power requirements of backscatter devices are not changed when $t=1$. For other time slots, the constraints are as follows:

$$\rho|h_k|^2\left((1-\tilde{\eta}_{k,l,k})P_{\max}+\sum_{t'=1}^{t-1}P_{\max}\right)\geq s_{k,l}(t)p_{\min},\quad k,l\in\mathcal{K}(t),\ 2\leq t\leq T, \tag{40}$$

$$\rho|h_l|^2\left((1-\tilde{\eta}_{k,l,l})P_{\max}+\sum_{t'=1}^{t-1}P_{\max}\right)\geq s_{k,l}(t)p_{\min},\quad k,l\in\mathcal{K}(t),\ 2\leq t\leq T. \tag{41}$$

These constraints ensure that the energy harvested in the previous time slots can be used for circuit operation of the backscatter devices in the current time slot. Similar to problem (39), the spectral efficiency in time slot t considering multi-slot energy causality constraints can be maximized using an iterative algorithm.

IV. Performance Evaluation

In this section, the performance of the proposed scheme is evaluated through simulations. The coverage area of the reader is considered as a cell with two ring-shaped boundary. The radii of inner and outer boundary are set to 10 m and 60 m, respectively. The backscatter devices are distributed randomly and uniformly in the coverage area of the reader. The path loss exponent α is equal to 2.5. The variance of the noise σ^2 is set to -100 dBm. The efficiency of the energy harvester ρ is set to 0.8 according to [26]. The results are obtained by averaging over different channel and path loss realizations.

We compare the performance of our proposed algorithm with the optimal scheme and five other schemes. In the optimal scheme, we obtain the global optimal transmit power of the reader using the Dinkelbach's algorithm. In each time slot, we use exhaustive search to find the backscatter device pairing that maximizes the energy efficiency. The optimal value of the reflection coefficients can be obtained from equations (52) and (56) in Appendix C. In the first scheme for comparison, we use genetic algorithm to solve the first subproblem. Given the reflection coefficients and backscatter device pairing, we maximize the average energy efficiency with respect to the transmit power of the reader using genetic algorithm. We use MATLAB genetic algorithm toolbox [37]. The second subproblem is solved using Dinkelbach's algorithm and SCA. The second scheme for comparison is the fixed device pairing scheme, we do not optimize backscatter device pairing. For device pairing, in each time slot, backscatter devices are sorted from the device with the strongest channel gain to the device with the weakest channel gain. Then, the first two backscatter devices are paired in the corresponding time slot. Furthermore, as inspired from [38], we consider the conventional device pairing scheme in which the backscatter device with the strongest channel gain is paired with the backscatter device with the weakest channel gain in each time slot. For the maximum transmit power allocation scheme, in each time slot, we set the transmit power of the reader to be equal to $P_{\max}$. In the random reflection coefficient selection scheme, the reflection coefficients of backscatter devices are chosen randomly. In this scheme, we only optimize the transmit power of the reader and backscatter device pairing. We note that in Figs. 5 to 9, the channel threshold for decoding the signal of backscatter devices γ is set to 0.

Fig. 5 shows the average energy efficiency over a superframe versus the number of iterations in Algorithm 3 for six settings: a) $K = 6$, $T = 3$, b) $K = 8$, $T = 4$, c) $K = 10$, $T = 5$, d) $K = 12$, $T = 6$ e) $K = 14$, $T = 7$, and f) $K = 16$, $T = 8$. The maximum transmit power of the reader $P_{\max}$ and the minimum circuit power requirement $p_{\min}$ are set to 35 dBm and -40 dB, respectively. As Fig. 5 shows, the alternating optimization algorithm converges very fast to a suboptimal solution of the average energy efficiency maximization problem. As it can be seen, the average energy efficiency converges after seven iterations. It is also shown that the average energy efficiency of backscatter system with NOMA increases with the number of backscatter devices in the system. This is because there are more degrees of freedom in backscatter device pairing and reflection coefficient selection when we increase the number of backscatter devices.

Fig. 6 shows the average energy efficiency versus the maximum transmit power of the reader $P_{\max}$. The number of backscatter devices K and minimum circuit power requirement $p_{\min}$ are set to 8 devices and -40 dB, respectively. As can be observed, the average energy efficiency of backscatter system with NOMA increases with the maximum transmit power

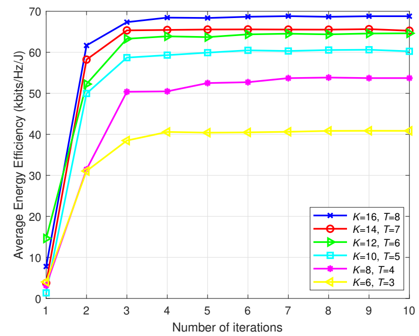

Fig. 5. Average energy efficiency over a superframe versus the number of iterations for different number of backscatter devices.

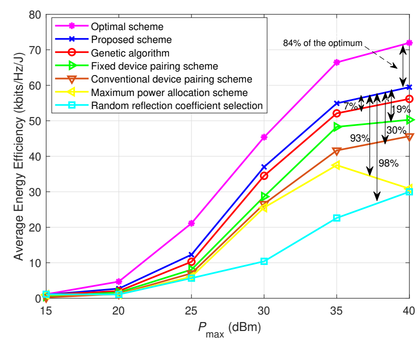

Fig. 6. Average energy efficiency versus the maximum transmit power of the reader.

of the reader and converges to the horizontal asymptote of its curve. For low values of $P_{\max}$, a large portion of power of incident carrier signal from the reader is harvested by the backscatter devices and a small portion of the power is reflected back to the reader. As a result, the data rate of backscatter devices decreases. Consequently, the average energy efficiency, which is the ratio of aggregate data rate to the amount of consumed power, decreases. When $P_{\max}$ increases, the aggregate data rate of backscatter devices improves and the average energy efficiency increases. The proposed scheme achieves an average energy efficiency that is within 84% of the optimal value. The gap between the average energy efficiency of the proposed scheme and optimal scheme is due to the fact that we used SCA to solve problem (22) in the alternating optimization algorithm. Thus, the proposed scheme provides a suboptimal solution for the average energy efficiency maximization problem. The average energy efficiency of five other schemes are also shown for comparison. As Fig. 6 shows, our proposed scheme achieves a 7% higher average energy efficiency than the scheme using the genetic algorithm. This is because the Dinkelbach's algorithm finds the global optimal solution for the transmit power of the reader while the genetic algorithm finds a local optimal solution for that. Our proposed scheme achieves a 19% higher average energy efficiency than the fixed device pairing scheme. Pairing the devices with the strongest channel gains improve the aggregate data rate. On the other hand, the amount of harvested energy increases. Thus, the average

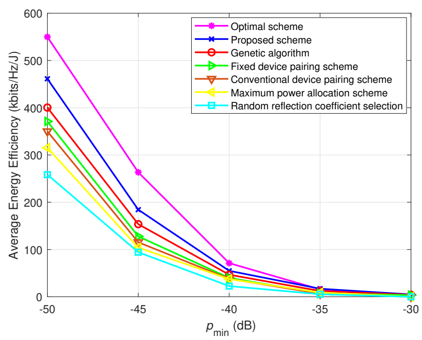

Fig. 7. Average energy efficiency versus the minimum power required for the circuit of backscatter devices p_{min}.

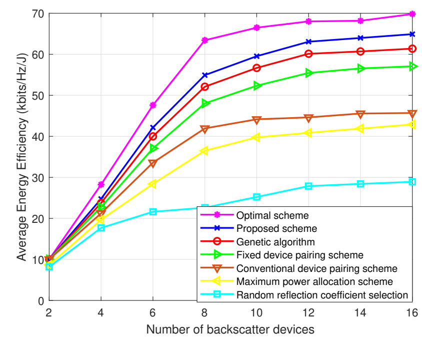

Fig. 8. Average energy efficiency versus the number of backscatter devices.

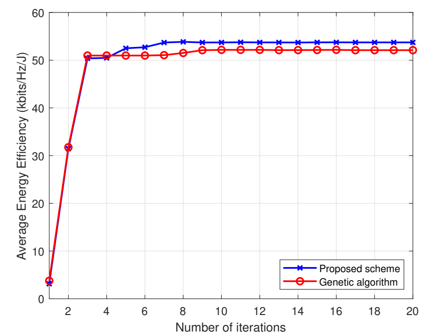

Fig. 9. Convergence of proposed algorithm and genetic algorithm.

energy efficiency degrades when compared with our scheme. Fig. 6 also shows that our proposed scheme increases the average energy efficiency by 30% when compared with the conventional device pairing scheme. Our proposed scheme has an average energy efficiency that is 93% higher than that of the maximum power allocation scheme. This is because the maximum power allocation increases the amount of harvested energy by the backscatter devices. As a result, the average energy efficiency of the system decreases. We also note that the average energy efficiency of the maximum power allocation scheme first increases with P_{max}, and then decreases. This is because both the aggregate data rate and consumed power increase with the maximum transmit power of the reader. But the increase in consumed power is much higher than that in the aggregate data rate. Thus, the energy efficiency degrades. Fig. 6 also shows the effect of optimizing the reflection coefficients on the average energy efficiency of the system. Results show that our proposed scheme increases the average energy efficiency by 98% when compared with the random reflection coefficient scheme.

Fig. 7 shows the effect of minimum power required for the circuit of backscatter devices on the average energy efficiency of the backscatter system. The number of backscatter devices K and P_{max} are set to 8 devices and 35 dBm, respectively. Results in Fig. 7 show that the average energy efficiency of backscatter system with NOMA decreases when we increase p_{min}. By increasing p_{min}, the amount of consumed power by backscatter devices increases. In addition, backscatter devices have to choose a lower value for the reflection coefficients to satisfy the minimum circuit power requirement for the backscatter devices. Consequently, the data rate of backscatter devices decreases and the average energy efficiency degrades. When the value of p_{min} is too high, the optimization problem is infeasible for most of the channel and path loss realizations with resulting average energy efficiency equal to zero. Fig. 7 also shows that our proposed scheme has a higher average energy efficiency than the baseline schemes. This is because of the global optimality of transmit power of the reader and optimizing pairing of backscatter devices as well as the transmit power of the reader and reflection coefficients, respectively.

Fig. 8 shows the average energy efficiency of the backscatter system with NOMA versus the number of backscatter devices. P_{max} and p_{min} are set to 35 dBm and -40 dB, respectively. The average energy efficiency increases with the number of backscatter devices. This is because the degrees of freedom for device pairing and reflection coefficient selection increase when there are more backscatter devices in Fig. 8 also shows that our proposed scheme achieves a higher average energy efficiency when compared with the baseline schemes.

Fig. 9 illustrates the convergence of proposed algorithms and genetic algorithm. The number of backscatter devices K and minimum circuit power requirement p_{min} are set to 8 devices and -40 dB, respectively. As it is shown in Fig. 9, the algorithms in both schemes converge to a suboptimal value for the average energy efficiency of the system. The rate of the convergence is similar for both schemes. The algorithms converge to a suboptimal solution in less than 10 iterations on average. We note that the computational complexity of Dinkelbach's algorithm which is used in our scheme, and the genetic algorithm is different. The complexity of solving the first subproblem using Dinkelbach's algorithm depends on the number of iterations in Dinkelbach's algorithm. The complexity of the genetic algorithm is in the order of multiplication of number of generations, population size, and the size of individuals in the algorithm. Our simulations by Intel Core i7-3770K 3.5 GHz CPU show that it takes 1 second on average to solve the first subproblem with Dinkelbach's algorithm while solving the first subproblem using the genetic algorithm requires 0.1 second on average.

Table I shows the average runtime of the proposed scheme

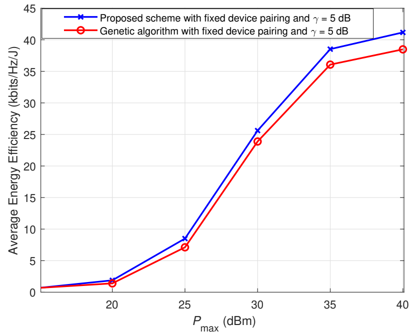

Fig. 10. Average energy efficiency versus the maximum transmit power of the reader for $\gamma = 5$ dB.

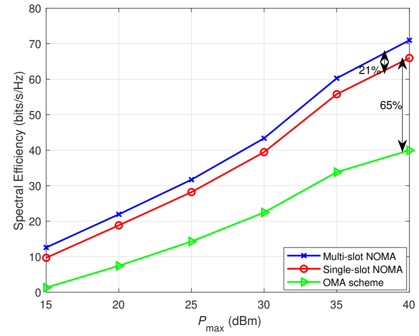

Fig. 11. Spectral efficiency versus the maximum transmit power of the reader.

TABLE I
RUNTIME OF THE ALGORITHMS (IN MINUTES)

Algorithm	$K = 4$	$K = 6$	$K = 8$	$K = 10$	$K = 12$
Proposed scheme	2.27	3.58	5.51	7.95	12.44
Optimal scheme	12.71	23.44	56.18	93.85	153.65

and the optimal scheme in minutes versus the number of backscatter devices for $P_{\max} = 35$ dBm. As shown in Table I, the runtime of the proposed scheme increases with the number of backscatter devices. In particular, when the number of backscatter devices changes from 10 to 12, the average runtime of the proposed scheme increases by 60%. The results also show that the runtime of the proposed scheme is less than that of the optimal scheme. In particular, when the number of backscatter devices is equal to 12, the runtime of the proposed scheme is 92% less than that of the optimal scheme.

Fig. 10 shows the average energy efficiency of the system versus the maximum transmit power of the reader for our proposed scheme and genetic algorithm, while the channel threshold for decoding the signal of backscatter devices γ is set to 5 dB. We consider that the device pairing is fixed. After sorting the backscatter devices according to their channel gains, backscatter devices with the strongest channel gains are paired in each time slot. We optimize the transmit power of the reader and reflection coefficients of backscatter devices using alternating optimization algorithm. As it is shown in Fig. 10, our proposed scheme achieves a higher average energy efficiency when compared with the scheme using genetic algorithm. By comparing Figs. 6 and 10, we note that the value of average energy efficiency of backscatter system with NOMA degrades when we increase γ from 0 dB to 5 dB. This is because the constraints on the SINR of backscatter devices limit the value of the reflection coefficients of multiplexing backscatter devices in each time slot. As a result, the harvested and consumed energy by the backscatter devices increase and the average energy efficiency of the system decreases.

Fig. 11 shows the spectral efficiency of NOMA backscatter system for $K = 8$ backscatter devices over a superframe. The minimum circuit power requirement is set to -40 dB. The spectral efficiency increases monotonically with the transmit power of the reader. This is because the SINR of the backscatter devices is improved when the maximum transmit power of the reader increases. Fig. 11 also shows the effect of multi-slot energy causality. Multi-slot energy causality increases the spectral efficiency of the system by 21% when compared with single slot energy causality. This is because a larger portion of carrier signal power is reflected back to the reader due to previously harvested power use. Fig. 11 also shows the spectral efficiency of backscatter system using OMA where at most one backsactter device operates on the subcarrier in each time slot. NOMA backscatter system achieves a spectral efficiency which is 65% higher than that of backscatter system with OMA. This is due to the orthogonal scheduling of the OMA scheme.

V. CONCLUSION

In this paper, we investigated a NOMA backscatter system, where signals from at most two backscatter devices are multiplexed on the frequency resource block using NOMA in each time slot. We formulated an average energy efficiency maximization problem by jointly optimizing the reflection coefficients, backscatter device pairing, and transmit power of the reader while taking the minimum circuit power and data rate requirements of the backscatter devices and the transmit power constraint of the reader into account. The formulated problem is nonconvex due to the nonconvexity of the objective function and the constraints. Using alternating optimization technique, we developed an algorithm to find a suboptimal solution. We decomposed the problem into two different subproblems with objective function in ratio form. The first subproblem is solved using concave-convex programming and Dinkelbach's algorithm. We used SCA and difference of convex programming to solve the second subproblem. By alternating optimization technique, the optimization variables are updated iteratively and alternatively until the average energy efficiency of the system converged to a suboptimal value. Simulation results showed that our proposed algorithm converged quickly to a suboptimal solution. Furthermore, our proposed algorithm achieves an average energy efficiency that is within 84% of the optimum. Runtime comparison showed that the runtime of the proposed scheme is less than that of the optimal scheme. Our scheme also increases the average energy efficiency of the system by 7%, 19%, 30%, 93%, and 98% when compared with the genetic algorithm, fixed device pairing scheme, conventional device pairing scheme, maximum transmit power allocation scheme, and random reflection coefficient selection scheme, respectively. In addition to the average energy efficiency, we studied the spectral efficiency of NOMA backscatter system subject to the single-slot and multi-slot energy causality constraints. Multi-slot energy causality increases the spectral efficiency of the system by 21% when compared with single-slot energy causality. We also showed that NOMA backscatter system achieves 65% higher spectral efficiency when compared with the OMA scheme. A potential extension for future work is to consider the average energy efficiency maximization in a backscatter system with MC-NOMA, where there are multiple subcarriers instead of one, and the signals from two backscatter devices are multiplexed on each subcarrier in one time slot.

Appendix

A. *Derivation of Constraints* (16d) *and* (16e)

From constraint (11i), we have

$$\log_2\left(1+\frac{\eta_k(t)P(t)g_k}{1+\eta_l(t)P(t)g_l}\right)\geq s_{k,l}(t)R_{\text{min}}. \tag{42}$$

For the case that $s_{k,l}(t)=0$, we must have $P(t)\geq 0$. For the case that $s_{k,l}(t)=1$, we have

$$\begin{aligned}\log_2\left(1+\frac{\eta_k(t)P(t)g_k}{1+\eta_l(t)P(t)g_l}\right)&\geq R_{\text{min}},\\ \frac{\eta_k(t)P(t)g_k}{1+\eta_l(t)P(t)g_l}&\geq 2^{R_{\text{min}}}-1. \end{aligned} \tag{43}$$

We define $\gamma=2^{R_{\text{min}}}-1$. From (43), we have

$$\begin{aligned}\eta_k(t)P(t)g_k&\geq\gamma+\gamma\eta_l(t)P(t)g_l,\\ P(t)(\eta_k(t)g_k-\gamma\eta_l(t)g_l)&\geq\gamma,\\ P(t)&\geq\frac{\gamma}{\eta_k(t)g_k-\gamma\eta_l(t)g_l}.\end{aligned} \tag{44}$$

By considering $s_{k,l}(t)$, we obtain

$$P(t)\geq\frac{s_{k,l}(t)\gamma}{\eta_k(t)g_k-\gamma\eta_l(t)g_l}. \tag{45}$$

From constraint (11j), we also have

$$\log_2\left(1+\eta_l(t)P(t)g_l\right)\geq s_{k,l}(t)R_{\text{min}}. \tag{46}$$

When $s_{k,l}(t)=0$, we can conclude $P(t)\geq 0$. When $s_{k,l}(t)=1$, we have

$$\begin{aligned}\log_2\left(1+\eta_l(t)P(t)g_l\right)&\geq R_{\text{min}},\\ P(t)&\geq\frac{2^{R_{\text{min}}}-1}{\eta_l(t)g_l},\\ P(t)&\geq\frac{\gamma}{\eta_l(t)g_l}.\end{aligned} \tag{47}$$

By considering $s_{k,l}(t)$, we have

$$P(t)\geq\frac{s_{k,l}(t)\gamma}{\eta_l(t)g_l}. \tag{48}$$

B. *Derivation of the First Term of (23a)*

We note that the first term in the objective function of (23) is another representation of (14). Here, we show how to obtain the first term of (23a). We have

$$\begin{aligned}&U_t(P(t),\boldsymbol{\eta}(t),\mathbf{s}(t))\\ &=\sum_{k\in\mathcal{K}(t)}\sum_{\substack{l\in\mathcal{K}(t)\\ l\neq k}}s_{k,l}(t)\Bigg(\log_2\left(1+\frac{\eta_k(t)P(t)g_k}{1+\eta_l(t)P(t)g_l}\right)\\ &\qquad+\log_2\left(1+\eta_l(t)P(t)g_l\right)\Bigg)\\ &=\sum_{k\in\mathcal{K}(t)}\sum_{\substack{l\in\mathcal{K}(t)\\ l\neq k}}s_{k,l}(t)\Bigg(\log_2\left(\frac{1+P(t)(\eta_k(t)g_k+\eta_l(t)g_l)}{1+\eta_l(t)P(t)g_l}\right)\\ &\qquad+\log_2\left(1+\eta_l(t)P(t)g_l\right)\Bigg)\\ &=\sum_{k\in\mathcal{K}(t)}\sum_{\substack{l\in\mathcal{K}(t)\\ l\neq k}}s_{k,l}(t)\Bigg(\log_2\Bigg(\frac{1+P(t)(\eta_k(t)g_k+\eta_l(t)g_l)}{1+\eta_l(t)P(t)g_l}\\ &\qquad\times(1+\eta_l(t)P(t)g_l)\Bigg)\Bigg)\\ &=\sum_{k\in\mathcal{K}(t)}\sum_{\substack{l\in\mathcal{K}(t)\\ l\neq k}}s_{k,l}(t)\left(\log_2\left(1+P(t)(\eta_k(t)g_k+\eta_l(t)g_l)\right)\right).\end{aligned} \tag{49}$$

C. *Derivation of the Optimal Reflection Coefficients*

From (10), we note that increasing the reflection coefficients of paired devices increases the energy efficiency in the corresponding time slot. According to constraints (13f) and (13g), the upper bound of the value of the reflection coefficients are as follows:

$$\eta_k(t)\leq 1-\frac{s_{k,l}(t)p_{\text{min}}}{\rho P(t)|h_k|^2},\ \ k,l\in\mathcal{K}(t), \tag{50}$$

$$\eta_l(t)\leq 1-\frac{s_{k,l}(t)p_{\text{min}}}{\rho P(t)|h_l|^2},\ \ k,l\in\mathcal{K}(t). \tag{51}$$

Furthermore, from (13h), we note that increasing the value of $\eta_k(t)$ increase the data rate of backscatter device k. Thus, for backscatter devices k and l that are paired in time slot t, i.e., $s_{k,l}(t)=1$, the optimal value of the reflection coefficient of device k in the optimal scheme can be obtained as follows:

$$\eta_k^*(t)=\max\left\{0,1-\frac{p_{\text{min}}}{\rho P(t)|h_k|^2}\right\}. \tag{52}$$

For $\eta_l(t)$, from constraint (13i), we have

$$\begin{aligned}\log_2\left(1+\eta_l(t)P(t)g_l\right)&\geq R_{\text{min}},\\ \eta_l(t)&\geq\frac{2^{R_{\text{min}}}-1}{P(t)g_l},\\ \eta_l(t)&\geq\frac{\gamma}{P(t)g_l}.\end{aligned} \tag{53}$$

Furthermore, from (13h), we have

$$\log_2\left(1+\frac{\eta_k^*(t)P(t)g_k}{1+\eta_l(t)P(t)g_l}\right)\geq R_{\text{min}},$$

$$\frac{\eta_k^*(t)P(t)g_k}{1+\eta_l(t)P(t)g_l} \geq 2^{R_{\min}}-1,$$
$$\eta_k^*(t)P(t)g_k \geq \gamma + \gamma\eta_l(t)P(t)g_l,$$
$$\eta_k^*(t)P(t)g_k - \gamma \geq \gamma\eta_l(t)P(t)g_l,$$
$$\frac{\eta_k^*(t)P(t)g_k-\gamma}{\gamma P(t)g_l} \geq \eta_l(t). \tag{54}$$

From (53) and (54), we can obtain the following inequality for the reflection coefficient of backscatter device l:

$$\frac{\gamma}{P(t)g_l} \leq \eta_l(t) \leq \frac{\eta_k^*(t)P(t)g_k-\gamma}{\gamma P(t)g_l}. \tag{55}$$

Thus, the optimal value of the reflection coefficient of backscatter device l in the optimal scheme can be obtained as follows:

$$\eta_l^*(t) = \max\left\{0, \min\left\{1-\frac{p_{\min}}{\rho P(t)|h_l|^2}, \frac{\eta_k^*(t)P(t)g_k-\gamma}{\gamma P(t)g_l}\right\}\right\}. \tag{56}$$

References

[1] N. Van Huynh, D. T. Hoang, X. Lu, D. Niyato, P. Wang, and D. I. Kim, "Ambient backscatter communications: A contemporary survey," *IEEE Communications Surveys & Tutorials*, vol. 20, no. 4, pp. 2889–2922, Fourth Quarter 2018.

[2] S. R. Islam, N. Avazov, O. A. Dobre, and K. S. Kwak, "Power-domain non-orthogonal multiple access (NOMA) in 5G systems: Potentials and challenges," *IEEE Communications Surveys & Tutorials*, vol. 19, no. 2, pp. 721–742, Second Quarter 2017.

[3] Z. Ding, X. Lei, G. K. Karagiannidis, R. Schober, J. Yuan, and V. K. Bhargava, "A survey on non-orthogonal multiple access for 5G networks: Research challenges and future trends," *IEEE J. Sel. Areas Commun.*, vol. 35, no. 10, pp. 2181–2195, Oct. 2017.

[4] J. Guo, X. Zhou, S. Durrani, and H. Yanikomeroglu, "Design of non-orthogonal multiple access enhanced backscatter communication," *IEEE Trans. Wireless Commun.*, vol. 17, no. 10, pp. 6837–6852, Oct. 2018.

[5] Q. Zhang, L. Zhang, Y. Liang, and P. Y. Kam, "Backscatter-NOMA: An integrated system of cellular and Internet-of-Things networks," in *Proc. of Int'l Conf. on Commun. (ICC)*, Shanghai, China, May 2019.

[6] A. Farajzadeh, O. Ercetin, and H. Yanikomeroglu, "UAV data collection over NOMA backscatter networks: UAV altitude and trajectory optimization," in *Proc. of IEEE Int'l Conf. on Commun. (ICC)*, Shanghai, China, May 2019.

[7] G. Yang, X. Xu, and Y. Liang, "Resource allocation in NOMA-enhanced backscatter communication networks for wireless powered IoT," *IEEE Wireless Commun. Letters*, vol. 9, no. 1, pp. 117–120, Jan. 2020.

[8] J. Wang, H. Ye, X. Kang, S. Sun, and Y. Liang, "Cognitive backscatter NOMA networks with multi-slot energy causality," *IEEE Communications Letters*, vol. 24, no. 12, pp. 2854–2858, Dec. 2020.

[9] F. Dashti Ardakani and V. W. S. Wong, "Joint reflection coefficient selection and subcarrier allocation for backscatter systems with NOMA," in *Proc. of IEEE Wireless Commun. and Networking Conf. (WCNC)*, May 2020.

[10] Y. Ye, L. Shi, R. Q. Hu, and G. Lu, "Energy-efficient resource allocation for wirelessly powered backscatter communications," *IEEE Communications Letters*, vol. 23, no. 8, pp. 1418–1422, Aug. 2019.

[11] S. Yang, Y. Deng, X. Tang, Y. Ding, and J. Zhou, "Energy efficiency optimization for UAV-assisted backscatter communications," *IEEE Communications Letters*, vol. 23, no. 11, pp. 2041–2045, Nov. 2019.

[12] H. Yang, Y. Ye, and X. Chu, "Max-min energy-efficient resource allocation for wireless powered backscatter networks," *IEEE Wireless Communications Letters*, vol. 9, no. 5, pp. 688–692, May 2020.

[13] L. Shi, R. Q. Hu, J. Gunther, Y. Ye, and H. Zhang, "Energy efficiency for RF-powered backscatter networks using HTT protocol," *IEEE Trans. on Vehicular Technology*, vol. 69, no. 11, pp. 13 932–13 936, Nov. 2020.

[14] Y. Xu, Z. Qin, G. Gui, H. Gacanin, H. Sari, and F. Adachi, "Energy efficiency maximization in NOMA enabled backscatter communications with QoS guarantee," *IEEE Wireless Commu. Lett.*, vol. 10, no. 2, pp. 353–357, Feb. 2021.

[15] A. A. Nasir, H. D. Tuan, T. Q. Duong, and M. Debbah, "NOMA throughput and energy efficiency in energy harvesting enabled networks," *IEEE Trans. on Communications*, vol. 67, no. 9, pp. 6499–6511, Sept. 2019.

[16] H. Zhang, M. Feng, K. Long, G. K. Karagiannidis, V. C. M. Leung, and H. V. Poor, "Energy efficient resource management in SWIPT enabled heterogeneous networks with NOMA," *IEEE Trans. on Wireless Communications*, vol. 19, no. 2, pp. 835–845, Feb. 2020.

[17] F. Fang, J. Cheng, and Z. Ding, "Joint energy efficient subchannel and power optimization for a downlink NOMA heterogeneous network," *IEEE Trans. Vehicular Technology*, vol. 68, no. 2, pp. 1351–1364, Feb. 2019.

[18] Y. Sun, D. W. K. Ng, Z. Ding, and R. Schober, "Optimal joint power and subcarrier allocation for MC-NOMA systems," in *Proc. of IEEE Global Commun. Conf. (GLOBECOM)*, Washington, DC, Dec. 2016.

[19] Y. Sun, D. W. K. Ng, Z. Ding, and R. Schober, "Optimal joint power and subcarrier allocation for full-duplex multicarrier non-orthogonal multiple access systems," *IEEE Trans. on Communications*, vol. 65, no. 3, pp. 1077–1091, Jan. 2017.

[20] D. Tse and P. Viswanath, *Fundamentals of Wireless Communication*. Cambridge University Press, 2005.

[21] W. Liu, K. Huang, X. Zhou, and S. Durrani, "Backscatter communications for Internet-of-Things: Theory and applications," *arXiv preprint arXiv:1701.07588*, Jan. 2017.

[22] J. F. Ensworth and M. S. Reynolds, "BLE-backscatter: Ultralow-power IoT nodes compatible with Bluetooth 4.0 low energy (BLE) smartphones and tablets," *IEEE Trans. on Microwave Theory and Techniques*, vol. 65, no. 9, pp. 3360–3368, Sep. 2017.

[23] G. Wang, F. Gao, W. Chen, and C. Tellambura, "Channel estimation and training design for two-way relay networks in time-selective fading environments," *IEEE Trans. on Wireless Communications*, vol. 10, no. 8, pp. 2681–2691, Aug. 2011.

[24] D. Mishra and E. G. Larsson, "Optimal channel estimation for reciprocity-based backscattering with a full-duplex MIMO reader," *IEEE Trans. on Signal Processing*, vol. 67, no. 6, pp. 1662–1677, Mar. 2019.

[25] Y. Xie, Z. Xu, S. Gong, J. Xu, D. T. Hoang, and D. Nyato, "Backscatter-assisted hybrid relaying strategy for wireless powered IoT communications," in *Proc. of IEEE Global Commun. Conf. (GLOBECOM)*, Waikoloa, HI, Dec. 2019.

[26] Y. Zou, J. Xu, S. Gong, Y. Guo, D. Niyato, and W. Cheng, "Backscatter-aided hybrid data offloading for wireless powered edge sensor networks," in *Proc. of IEEE Global Commun. Conf. (GLOBECOM)*, Waikoloa, HI, Dec. 2019.

[27] W. Ma, W. Wang, and T. Jiang, "Energy beamforming for wireless information and power transfer in backscatter multiuser networks," in *Proc. of IEEE Global Commun. Conf. (GLOBECOM)*, Waikoloa, HI, Dec. 2019.

[28] C. Huang, A. Zappone, G. C. Alexandropoulos, M. Debbah, and C. Yuen, "Reconfigurable intelligent surfaces for energy efficiency in wireless communication," *IEEE Trans. Wireless Commun.*, vol. 18, no. 8, pp. 4157–4170, Jun. 2019.

[29] K. Shen and W. Yu, "Fractional programming for communication systems - Part I: Power control and beamforming," *IEEE Trans. on Signal Processing*, vol. 66, no. 10, pp. 2616–2630, May 2018.

[30] ——, "Fractional programming for communication systems - Part II: Uplink scheduling via matching," *IEEE Trans. on Signal Processing*, vol. 66, no. 10, pp. 2631–2644, May 2018.

[31] S. Guo, Y. Shi, Y. Yang, and B. Xiao, "Energy efficiency maximization in mobile wireless energy harvesting sensor networks," *IEEE Trans. on Mobile Computing*, vol. 17, no. 7, pp. 1524–1537, Jul. 2017.

[32] A. Zappone, E. Björnson, L. Sanguinetti, and E. Jorswieck, "Globally optimal energy-efficient power control and receiver design in wireless networks," *IEEE Trans. on Signal Processing*, vol. 65, no. 11, pp. 2844–2859, Jun. 2017.

[33] W. Dinkelbach, "On nonlinear fractional programming," *Management Science*, vol. 13, no. 7, pp. 492–498, Mar. 1967.

[34] M. Grant and S. Boyd, *CVX: Matlab software for disciplined convex programming*, 2020. [Online]. Available: http://cvxr.com/cvx/

[35] S. Boyd and L. Vandenberghe, *Convex Optimization*. Cambridge University Press, 2004.

[36] A. Ben-Tal and A. Nemirovski, *Lectures on Modern Convex Optimization: Analysis, Algorithms, and Engineering Applications*. SIAM, 2001.

[37] A. J. Chipperfield and P. J. Fleming, "The MATLAB genetic algorithm toolbox," in *Proc. of IEE Colloquium on Applied Control Techniques Using MATLAB*, London, UK, Jan. 1995.

[38] Z. Ding, P. Fan, and H. V. Poor, "Impact of user pairing on 5G nonorthogonal multiple-access downlink transmissions," *IEEE Trans. on Vehicular Technology*, vol. 65, no. 8, pp. 6010–6023, Aug. 2016.

Farhad Dashti Ardakani (S'19) received the B.Sc. degree from University of Tehran, Tehran, Iran, in 2017, and the M.A.Sc. degree from the University of British Columbia (UBC), Vancouver, BC, Canada, in 2020. His main research interests include non-orthogonal multiple access (NOMA), backscatter communication systems, optimization for wireless communication networks, and machine learning. He was awarded the University of Tehran Foundation scholarship as an honor student during his bachelor program. Currently, he is working as an Associate Engineer Intern at Huawei, Ottawa, ON, Canada.

Rui Huang (S'19) received the B.Eng. degree from Chongqing University, Chongqing, China, in 2015, and the M.Eng. degree from Shanghai Jiao Tong University (SJTU), Shanghai, China, in 2018. He is currently a Ph.D. Candidate in the Department of Electrical and Computer Engineering, The University of British Columbia (UBC), Vancouver, Canada. He has been a recipient of the Four Year Doctoral Fellowship (4YF) at UBC since 2018. His research interests include Internet of Things (IoT) and machine learning for optimization in wireless communication systems.

Vincent W.S. Wong (S'94, M'00, SM'07, F'16) received the B.Sc. degree from the University of Manitoba, Winnipeg, MB, Canada, in 1994, the M.A.Sc. degree from the University of Waterloo, Waterloo, ON, Canada, in 1996, and the Ph.D. degree from the University of British Columbia (UBC), Vancouver, BC, Canada, in 2000. From 2000 to 2001, he worked as a systems engineer at PMC-Sierra Inc. (now Microchip Technology Inc.). He joined the Department of Electrical and Computer Engineering at UBC in 2002 and is currently a Professor. His research areas include protocol design, optimization, and resource management of communication networks, with applications to wireless networks, smart grid, mobile edge computing, and Internet of Things. Currently, Dr. Wong is the Chair of the Executive Editorial Committee of *IEEE Transactions on Wireless Communications*, an Area Editor of *IEEE Transactions on Communications* and *IEEE Open Journal of the Communications Society*, and an Associate Editor of *IEEE Transactions on Mobile Computing*. He has served as a Guest Editor of *IEEE Journal on Selected Areas in Communications*, *IEEE Internet of Things Journal*, and *IEEE Wireless Communications*. He has also served on the editorial boards of *IEEE Transactions on Vehicular Technology* and *Journal of Communications and Networks*. He was a Tutorial Co-Chair of *IEEE GLOBECOM*'18, a Technical Program Co-chair of *IEEE VTC*2020-*Fall* and *IEEE SmartGridComm*'14, as well as a Symposium Co-chair of *IEEE ICC*'18, *IEEE SmartGridComm* ('13, '17) and *IEEE GLOBECOM*'13. He is the Chair of the IEEE Vancouver Joint Communications Chapter and has served as the Chair of the IEEE Communications Society Emerging Technical Sub-Committee on Smart Grid Communications. He was an IEEE Communications Society Distinguished Lecturer (2019 - 2020).